

# POLITECNICO DI TORINO

Master's Degree in Mechatronics Engineering



## Design of the Power System for an Autonomous Hybrid Wing-In Ground Effect Vehicle

Commercial and Military Applications

Supervisors

Prof. Iustin Radu Bojoi

Prof. Sergio Dominguez

Candidate

Riccardo Pasquino

October 2024

## Abstract

The shift towards more-electric and autonomous vehicles in electric-mobility applications requires innovative energy management strategies, especially for hybrid systems that integrate fuel cells, batteries and supercapacitors.

Wing In Ground (WIG) effect vehicles represent both a significant challenge and a promising opportunity for the development of future hybrid-electric vehicles. Their capability to achieve high speeds with low energy consumption by exploiting the ground effect meets mobility requirements while allowing functionality without the need for specialized infrastructure.

The combination of the power-electronic components in the hybrid system allows a variety of possible configurations that can be tailored to specific mission requirements, this aspect makes them versatile and efficient. Among these configurations, the most complex and studied is the one involving fuel cells, batteries and supercapacitors. These energy sources are managed through Energy Management System (EMS) strategies, which differ based on how they distribute energy among the sources in different operational scenarios. The study explores several EMS strategies, including the State Machine, Classical Proportional Integral (PI), Fuzzy Logic, Frequency Decoupling, Equivalent Consumption Minimization Strategy (ECMS) and External Energy Maximization Strategy (EEMS). A new strategy, the Memory-based Hysteresis PI (MH-PI), was developed to address some identified shortcomings in these previous ones.

To optimize the use of EMS strategies, it is essential to manage energy sources through converters, which inherently introduce inefficiencies. A balanced approach was identified in a topology that incorporates a DC/DC converter for fuel cells, a bidirectional DC/DC converter for the battery and a necessary DC/AC converter to connect the load. The strategies mainly differ for the Fuel Cell Power computation, instead, the battery power is managed by a PI controller in order to keep the desired bus voltage.

Field tests with scale models provided valuable data, particularly for the takeoff phase, which is one of the most demanding in terms of system response speed and power request. The most valuable result is the discovery of a characteristic takeoff profile for WIG vehicles, marked by an initial power peak, followed by stabilisation at approximately one-fifth of the peak power. This profile was used to simulate the takeoff manoeuvre, one of the most challenging scenarios for the EMS.

Simulations were conducted on Simulink, using the Simscape Power Systems add-on thanks to its wide power-electronic components library. All strategies have been tested using a typical takeoff and stabilization load pattern of about

10 minutes. The results were compared based on components' wear and tear, fuel consumption, efficiency and reaction slope.

The ECMS strategy offers the best reaction time but results in the highest fuel consumption. On the other hand, the EEMS strategy achieved the lowest hydrogen usage while maintaining good reaction time and efficiency. However, this strategy had to be discarded due to fluctuations during steady-state operation, which caused stress and wear on the components. Among all the strategies tested, the MH-PI emerged as the best compromise, balancing the key parameters effectively and offering a promising solution for managing energy in WIG vehicles.



# Acknowledgements



# Table of Contents

<b>List of Tables</b>	VI
<b>List of Figures</b>	VII
<b>Acronyms</b>	X
<b>1 Introduction</b>	2
1.1 Origins of Wing-in Ground Effect Vehicles . . . . .	3
1.2 Physics of the Ground Effect . . . . .	6
1.3 WIG Vehicles Characteristics . . . . .	8
1.3.1 Pro . . . . .	8
1.3.2 Contra . . . . .	9
<b>2 Power System</b>	10
2.1 Configuration . . . . .	11
2.2 Topology . . . . .	12
2.2.1 One unidirectional DC/DC converter for Fuel Cells and two bidirectional DC/DC converters for Battery and Supercapacitors . . . . .	13
2.2.2 One unidirectional DC/DC converter for Fuel Cells and one bidirectional DC/DC converter for Battery and Supercapacitors	14
2.2.3 One unidirectional DC/DC converter for Fuel Cells and one bidirectional DC/DC converter for Battery . . . . .	15
2.2.4 One unidirectional DC/DC converter for Fuel Cells and two bidirectional DC/DC converter for Supercapacitors . . . . .	16
2.2.5 One unidirectional DC/DC converter for Fuel Cells . . . . .	17
2.3 System Sizing . . . . .	18
2.3.1 Fuel Cells . . . . .	19
2.3.2 Batteries . . . . .	19
2.3.3 Supercapacitors . . . . .	20
2.3.4 Power System Characteristics . . . . .	22

2.4	Components . . . . .	22
2.4.1	Fuel Cells . . . . .	22
2.4.2	Battery . . . . .	23
2.4.3	Supercapacitors . . . . .	24
<b>3</b>	<b>Energy Management System Strategies</b>	<b>26</b>
3.1	General Working Principle . . . . .	26
3.2	Strategies Description . . . . .	28
3.2.1	State Machine Control Strategy . . . . .	28
3.2.2	Classical PI Control Strategy . . . . .	30
3.2.3	Rule Based Fuzzy Logic Control Strategy . . . . .	31
3.2.4	Frequency Decoupling and State Machine Control Strategy .	36
3.2.5	Equivalent Consumption Minimization Strategy . . . . .	36
3.2.6	External Energy Maximization Strategy . . . . .	36
3.3	Memory-Based Hysteresis PI Control Strategy . . . . .	37
<b>4</b>	<b>Typical Take-off Load Pattern</b>	<b>40</b>
<b>5</b>	<b>Simulation Details</b>	<b>43</b>
5.1	Load . . . . .	45
5.2	Parameters Setting . . . . .	47
5.3	Strategies Settings . . . . .	48
<b>6</b>	<b>Simulation Results</b>	<b>49</b>
6.1	Power Scopes . . . . .	49
6.2	Key-Parameters . . . . .	54
6.3	Observations . . . . .	55
<b>7</b>	<b>Conclusions</b>	<b>57</b>
7.1	Commercial Applications . . . . .	58
7.2	Military Applications . . . . .	58
<b>8</b>	<b>Future Work</b>	<b>60</b>
<b>A</b>	<b>Field Tests Scale Models Details</b>	<b>63</b>
<b>B</b>	<b>Components Datasheets</b>	<b>66</b>
B.1	Fuel Cell . . . . .	66
B.2	Solid State Battery . . . . .	67
B.3	Supercapacitors . . . . .	70
	<b>Bibliography</b>	<b>73</b>

# List of Tables

2.1	Main characteristics of a scale model take-off typical load pattern . . . . .	18
2.2	Energy system requirements . . . . .	22
3.1	State Machine Control: rule-based state transition diagram . . . . .	29
6.1	Simulation strategies comparison - key-parameters results . . . . .	55

# List of Figures

1.1	787 electrical system architecture differences with a traditional aircraft	3
1.2	Toivo Kaairo with the single fan prototype powered by a motorcycle engine, 1930s . . . . .	4
1.3	Military hovercraft, 1990s . . . . .	4
1.4	Korabl Maket, also known as Caspian Sea Monster, 1960s . . . . .	5
1.5	S31-Lun Class, 1980s . . . . .	5
1.6	WidgetWorks - AirFish 8 . . . . .	6
1.7	Ground effect physics scheme . . . . .	7
1.8	Fit curve of the relationship between reduced drag and flight altitude	8
2.1	Topology study schemes (a) . . . . .	13
2.1	Topology study schemes (b) . . . . .	14
2.1	Topology study schemes (c) . . . . .	15
2.1	Topology study schemes (d) . . . . .	16
2.1	Topology study schemes (e) . . . . .	17
3.1	Battery converters control scheme . . . . .	27
3.2	Classical PI Simulink scheme . . . . .	31
3.3	Matlab Toolbox - Fuzzy Logic Designer (a) . . . . .	32
3.3	Matlab Toolbox - Fuzzy Logic Designer (b) . . . . .	32
3.3	Matlab Toolbox - Fuzzy Logic Designer (c) . . . . .	33
3.3	Matlab Toolbox - Fuzzy Logic Designer (d) . . . . .	33
3.3	Matlab Toolbox - Fuzzy Logic Designer (e) . . . . .	34
3.3	Matlab Toolbox - Fuzzy Logic Designer (f) . . . . .	34
3.3	Matlab Toolbox - Fuzzy Logic Designer (g) . . . . .	35
3.4	Operation Scheme - Classical PI (left) / Modified PI (right) <b>1:</b> Battery delivers its Max Power while from Fuel Cells is required the Power to meet the Load <b>0:</b> Fuel Cells deliver the Power necessary to satisfy the load requirement and to recharge the Battery . . . . .	38
3.5	PI control scheme . . . . .	39

4.1	Mistral - 1.5m wingspan scale model . . . . .	40
4.2	Albatros - 2m wingspan scale model . . . . .	40
4.3	Field test data - Power Demand (Blue) / Current (Red) / Voltage (Green) . . . . .	42
5.1	Original simulation . . . . .	44
5.2	Typical take-Off load pattern - filtered . . . . .	45
5.3	Lookup tables load profile - 5 mins(up) / 10 mins (down) . . . . .	46
5.4	Simulink initialization function . . . . .	47
5.5	MH-PI switches configuration scheme . . . . .	48
6.1	Power Scope - State Machine Control . . . . .	50
6.2	Power Scope - Frequency Decoupling and State Machine Control . .	50
6.3	Power Scope - Classical PI Control . . . . .	51
6.4	Power Scope - Memory-Based Hysteresis PI Control . . . . .	51
6.5	Power Scope - Fuzzy Logic Control . . . . .	52
6.6	Power Scope - Equivalent Consumption Minimization Strategy . . .	52
6.7	Power Scope - External Energy Maximization Strategy . . . . .	53
A.1	Albatros dimensional details . . . . .	63
A.2	Albatros hardware components details . . . . .	64
A.3	Mistral datasheet . . . . .	65
B.1	H-Series fuel cell stacks / H-3000 datasheet . . . . .	66
B.2	High Performance Battery - SSB datasheet, page 1/3 . . . . .	67
B.3	High Performance Battery - SSB datasheet, page 2/3 . . . . .	68
B.4	High Performance Battery - SSB datasheet, page 3/3 . . . . .	69
B.5	SCX5000 datasheet, page 1/2 . . . . .	70
B.6	SCX5000 datasheet, page 2/2 . . . . .	71



# Acronyms

**GEV**

Ground Effect Vehicle

**WIGE**

Wing-In Ground Effect

**WIG**

Wing-In Ground

**RAE**

Ram Air Effect

**MEA**

More Electric Aircraft

**EMS**

Energy Management System

**FC**

Fuel Cells

**SC**

SuperCapacitors

**B**

Battery

**SOC**

State Of Charge

**SSB**

Solid State Battery

**EV**

Electric Vehicle

**ESR**

Equivalent Series Resistance

**HPB**

High Performance Battery

**LiBs**

Lithium-ion Batteries

**ECMS**

Equivalent Consumption Minimization Strategy

**EEMS**

External Energy Maximization Strategy

**MH-PI**

Memory-Based Hysteresis Proportional Integral Control

**FIS**

Fuzzy Inference System

# List of Symbols

$\chi$	Scale Factor
$\eta$	Converter efficiency
$\eta_{sys}$	Overall System Efficiency
$C_{batt,tot}$	Battery Capacity considering DOD
$C_{batt}$	Battery Capacity
$C_{sc,scale}$	Supercapacitors Capacity considering DOD and $\chi$
$C_{sc,tot}$	Supercapacitors Capacity considering DOD
$C_{sc}$	Supercapacitors Capacity
$DOD$	Depth of Discharge
$P_{b,char}$	Battery Charging Power
$P_{batt,max}$	Battery Maximum Power
$P_b$	Instantaneous Battery Output Power
$P_{fc,max}$	Fuel Cells Maximum Power
$P_{fc,min}$	Fuel Cells Minimum Power
$P_{fc,nominal}$	Fuel Cells Nominal Power
$P_{fc,opt}$	Optimal Fuel Cell Power
$P_{fc}$	Instantaneous Fuel Cells Output Power
$P_{load}$	Instant Power Demand

$P_{mean}$	Load Average Power
$P_{pre-roll}$	Load Pre-Rolling Power
$P_{sc,max}$	Supercapacitors Maximum Power
$P_{sc}$	Instantaneous Supercapacitors Output Power
$V_{dc,bus}$	Common Bus Voltage
$V_{dc,ref}$	Common Bus Desired Voltage
$P_{max,cont}$	Load Max Continuous Mode Power
$P_{peak}$	Load Peak Power
$P_{trans}$	Load Transient Peak Power
$t_{op}$	Load Operational Time
$t_{trans}$	Load Transient Time



# Chapter 1

## Introduction

In a world increasingly strained by pollution, exploitation and disregard for the environment, eco-friendly solutions are of paramount importance. These also bring with them new technologies with excellent technical features that can be employed to create increasingly high-performance devices.

The aviation industry has seen growing interest in the electrification of aircraft over the last few decades. A concept known as the More Electric Aircraft (MEA) phenomenon, focuses on increasing the electrification of aircraft systems. The aviation industry has used electric systems for certain components for many decades, particularly for communication, lighting and navigation. However, major systems such as hydraulics and pneumatics still dominated the power architecture of aircraft.

The MEA concept started to emerge in the 1980s when engineers began investigating how to reduce the reliance on hydraulic, pneumatic, and mechanical systems in favor of electrical systems. The term "More Electric Aircraft" began to formalize during the 1990s, driven by the realization that electrical systems could offer substantial benefits over traditional systems, the idea was to replace heavy pneumatic and hydraulic systems reducing aircraft weight, thereby improving fuel efficiency. During the 2000s, the electrification process accelerated due to a growing awareness of the importance of the previously mentioned factors, along with the added benefits of reduced maintenance costs and increased recognition of pollutant gases as key contributors to climate change. [1]

The phenomenon, right after the scientific research phase, found its way into the commercial sphere with the Boeing 787 Dreamliner (Fig.1.1)[2] and into the military sphere with the F-35 lightning II which, in addition to the conversion of hydraulic-mechanical systems to electrical, addressed the electrical power required by mission-specific components such as flight systems and sensors such as the Electro-Optical Targeting System (EOTS) [3]

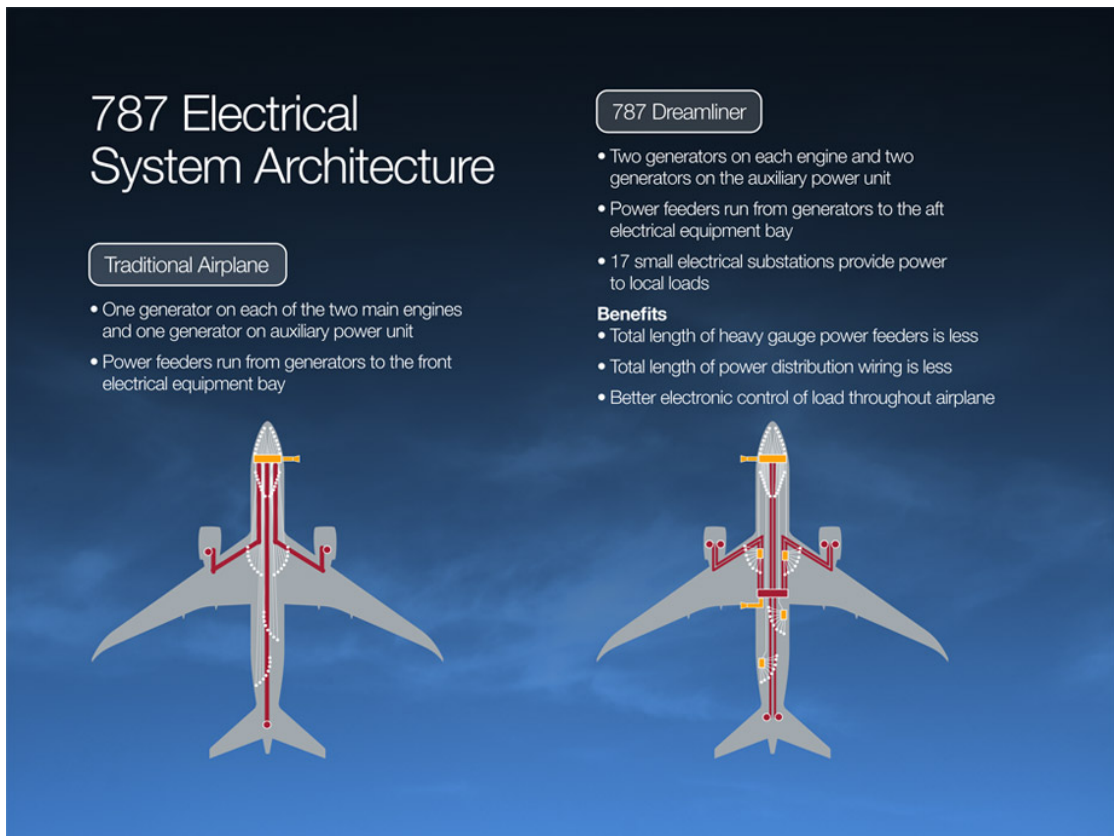


**Figure 1.1:** 787 electrical system architecture differences with a traditional aircraft

In the wake of this trend, the development of aircraft electrification technologies is proceeding at a great pace. Nowadays, companies such as Airbus, Boeing and other startups are targeting the development of all-electric midsize aircraft.

Regardless, today's aircraft, although undergoing continuous improvement, represent a large consumption of energy, no matter from what source it is produced from. To overcome this problem are the Wing-In Ground (WIG) vehicles, which, with their features, potentially represent a revolution in the world of transportation.

## 1.1 Origins of Wing-in Ground Effect Vehicles

The Wing-in Ground effect (WIGE) vehicles belong to a wider category of Ground Effect Vehicles (GEVs). These type of crafts exploit the Ground Effect to reduce the drag with air and fly, or float, over the land in order to obtain adaptability to different ground type and improved energy efficiency. The first study of such vehicles can be addressed to John Thornycroft when in 1877 tested a modified

boat, the concept was to pump air under the hull in order to reduce to drag and achieve better velocities. At that time the available technology was not enough to fully exploit Thornycroft's idea. Luckily in the future other scientists like Dagobert Müller von Thomamühl and Toivo Kaario(Figure 1.2)[4] have continued to develop similar vehicles resulting in today's Hovercraft (Figure 1.3).



**Figure 1.2:** Toivo Kaario with the single fan prototype powered by a motorcycle engine, 1930s



**Figure 1.3:** Military hovercraft, 1990s

Hovercrafts exploit ground effect to lift the machine over a cushion of air created by downward-facing fans. This led to the possibility to use them over multiple surfaces like:

- land
- brushwood
- mud
- water
- ice
- snow

Due to their versatility, hovercrafts are well suited for both military and commercial applications. However, they lack in velocity and fuel efficiency. In contrast, Wing-In-Ground (WIG) vehicles can achieve high speeds with low energy consumption.

In the late 1920s, the first flights of the Dornier Do X, a Swiss seaplane, demonstrated how flying close to the water's surface significantly extended its range. However, the most significant advancements in WIG vehicles came from Rostislav Alexeyev, part of the Russian Central Hydrofoil Design Bureau. These vehicles, also known as ekranoplans, were primarily developed for military purposes during the Cold War. For this reason, much of the technical information about ekranoplans remains classified.

Rostislav, the creator of the SM-1 and SM-2, introduced innovative features, such as positioning jet engines at the front of the aircraft to use exhaust gases to increase wing lift. This design, together with the other innovations, led to the development of the "Korabl Maket" better known as the Caspian Sea Monster (Figure 1.4), which boasted remarkable performance, including a cruising speed of 430 km/h and a range of 1,500 km. Despite its potential, the Caspian Monster never entered active service. However, it laid the groundwork for the Lun-Class ekranoplan.

The Lun-Class ekranoplan, specifically the S-31 model (Figure 1.5), achieved a range of 2,000 km at speeds exceeding 370 km/h and could carry a payload of up to 137,000 kg. It was equipped with 6 cruise missiles and its ability to fly close to the surface made it invisible to both sonar and radar. This allowed it to enter service in the Soviet Navy during the 1980s.

In the late 1980s, the fall of the Soviet Union and high maintenance costs led to the decommissioning of the S-31, along with the decline in WIG technology development.

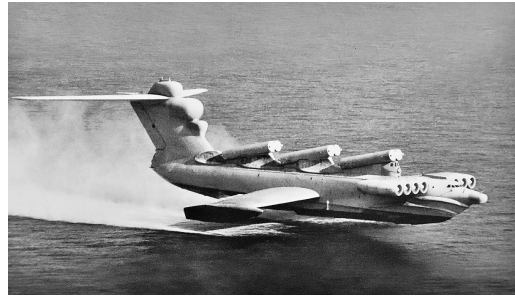


**Figure 1.4:** Korabl Maket, also known as Caspian Sea Monster, 1960s      **Figure 1.5:** S31-Lun Class, 1980s

Only at the beginning of the 21st century a renewed attention arose as new technologies and materials became available, making WIG vehicles more practical for commercial, recreational, and military applications. For example, the AirFish 8 (Figure 1.6) is a unique marine vessel that operates using Wing-in-Ground (WIG) effect technology. Developed by the Singapore-based company Wigetworks[5], the

AirFish 8 is designed for fast coastal transport and can reach speeds of up to 90 knots (about 167 km/h). The AirFish 8 offers a futuristic transportation solution, combining the speed of aircraft with the simplicity and efficiency of water vessels, particularly for regions with multiple islands or coastal areas.



Figure 1.6: WigetWorks - AirFish 8

## 1.2 Physics of the Ground Effect

The ground effect, in aviation, is a phenomenon where an aircraft experiences increased lift and reduced drag when flying close to the ground, in the range of about one wingspan. This is mainly caused by two factors[4]:

- **Ram Air Effect (RAE):** this effect occurs when air is forced into an intake, in this case the space between the wings and the ground. The results is an augmented lift due to the stagnation overpressure.
- **Wing Aspect Ratio Effect:** Long and narrow wings (high aspect ratio) generally result in less induced drag and greater efficiency. However, in order to better harness the ground effect and withstand the significant stresses they are subjected to, WIG vehicles require shorter and wider wings (low aspect ratio). In either case, they experience an outward flow caused by the ground effect, which pushes vortexes away from the wing that would otherwise be forced back down (Figure 1.7).

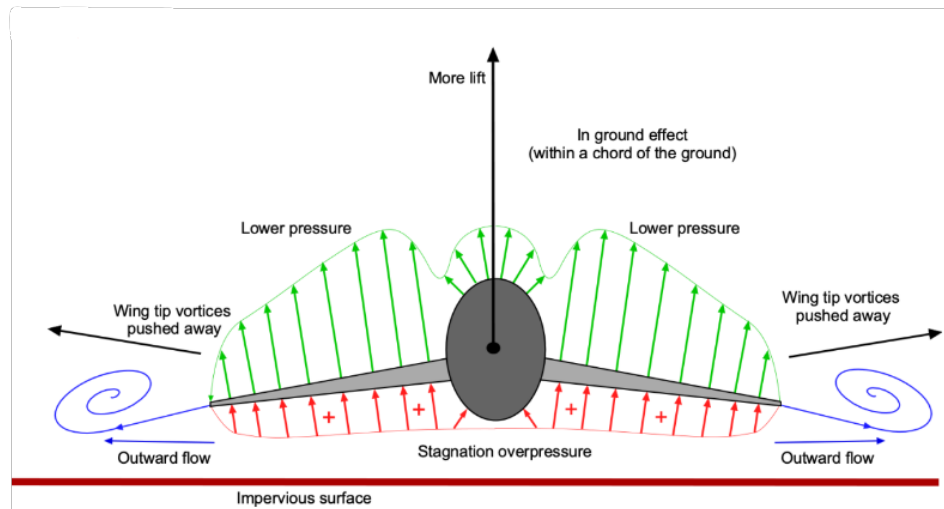
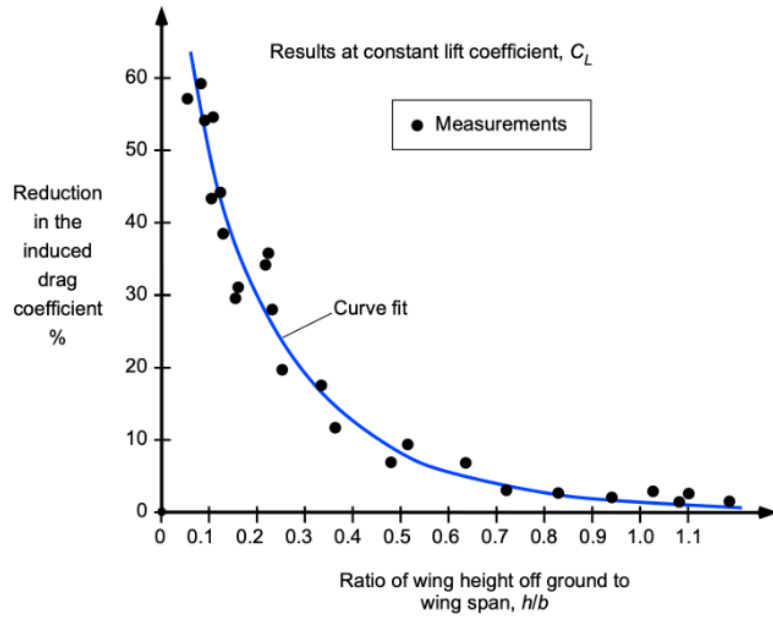


Figure 1.7: Ground effect physics scheme

WIG vehicles require special consideration during the design process, as additional factors beyond those previously discussed must be addressed. Two key aspects are:

- **Large tail horizontal control surface** to counteract the instability that arises when the aircraft exits the Ground-Effect zone, due to changes in pitching moment.
- **Wing-tip floats** which provide stability when the craft is in water, as well as during take-off and flight, to better capture the ground effect.

As previously said aircrafts benefit from ground effect when flying in an altitude range of about a wingspan, as can be deduced from the Figure 1.8 [4], however, there is a significant increase in benefit in the range below half the wingspan.



**Figure 1.8:** Fit curve of the relationship between reduced drag and flight altitude

This is a crucial factor, as flying close to the surface offers several beneficial aspects, such as enhanced lift and reduced drag. However, this altitude also poses significant risks, particularly regarding potential hazards encountered over the water surface. These hazards can include buoys, fishing nets, debris and waves, all of which necessitate careful navigation and awareness from the pilot or autonomous control systems to ensure safe operation.

## 1.3 WIG Vehicles Characteristics

As outlined above, WIG vehicles offer many advantages; however, it is equally important to consider their drawbacks.

### 1.3.1 Pro

- high speed
- high efficiency
- high payload
- long operational range
- no radar/sonar detection

### **1.3.2 Contra**

- instability in the transition out the ground effect zone
- need for relatively smooth surface during flight

The instability caused by changes in the pitching moment is a critical factor to consider, both for safety reasons and due to the challenge of developing a robust controller for an unmanned vehicle capable of handling this condition.

Regarding the need for smooth surfaces, certain projects, such as the DARPA [6] initiative, are working to overcome this limitation by expanding the use of WIG vehicles to rough seas, though with potentially reduced efficiency.

In conclusion, while WIG vehicles offer a promising future, they still face significant challenges.

## Chapter 2

# Power System

In response to the growing demand for eco-friendly aviation solutions, a range of innovative technologies has emerged to meet sustainability goals. Modern power systems now incorporate a variety of advanced components that can be configured in various ways to optimize performance. These systems are not limited to 100% electric solutions; instead, hybrid approaches are increasingly garnering attention. Technologies such as fuel cells, batteries and advanced electric propulsion systems can be integrated, with each contributing unique advantages. For instance, fuel cells offer an effective solution for extending operational range, complementing the capabilities of fully electric systems. By combining different power sources, it is possible to create flexible, efficient and environmentally sustainable configurations for future aircraft.

The development and implementation of power systems for Wing-in-Ground Effect (WIG) vehicles are relatively under-explored areas due to the scarcity of available data and the relatively recent trend towards electrification. Consequently, there is a lack of comprehensive studies on power systems specifically designed for WIG vehicles. Nevertheless, general information from the field of e-mobility can provide a valuable starting point. For instance, the work "A Fuel Cell Hybrid Emergency Power System for a More Electric Aircraft" [7] serves as a solid foundation for analysis and simulations.

## 2.1 Configuration

To maximize the benefits of Energy Management Strategies (EMS), it's essential to differentiate the power contributions from multiple energy sources and leverage the strengths of each component. The primary components used in hybrid power systems include:

- **Fuel Cell (FC):** Fuel cells generate electricity by converting chemical energy from hydrogen or other fuels. They are crucial because they provide clean, efficient power with minimal emissions and can deliver a high amount of power, making them suitable for heavy-duty applications and long-duration use in hybrid systems.
- **Battery (B):** Batteries store electrical energy and release it when needed. They are vital for energy storage in hybrid systems, providing steady power output and acting as a buffer during periods of high demand or low energy generation.
- **Supercapacitors (SC):** Supercapacitors store and discharge energy rapidly. This fast response is essential in systems like aircraft, where quick bursts of power are needed for acceleration, maneuvering, or sudden changes in load. Their ability to handle high power surges ensures system stability during critical moments.
- **Electric Motor:** The electric motor converts electrical energy into mechanical energy, driving propulsion systems. It is essential for green solutions in hybrid power systems due to its high efficiency and ability to reduce emissions. In aircraft, electric motors help in providing cleaner propulsion alternatives, contributing to the shift towards more sustainable and eco-friendly aviation.
- **Power Electronics:** Power electronics manage and control the flow of electrical energy between components, ensuring optimal performance and efficiency. They are crucial for integrating multiple energy sources and ensuring smooth transitions between them, maximizing overall system performance.
- **Flywheel:** The flywheel, in particular, has been studied for its potential in the electrification process due to its ability to recover energy that would otherwise be lost and its notable energy density (1.26 kW/kg nominal and 18 kW/kg peak) [8]. While there are a few papers on e-mobility applications for Flywheel Energy Storage Systems (FESS) [8, 9, 10], most research focuses on stationary applications like charging points and green energy production improvements [11, 12, 13, 14]. For the purposes of this study, the flywheel will be acknowledged but considered as a topic for future research due to the already high complexity of the current scope.

The combination of these components enables a wide range of maneuverability for EMS strategies. Additionally, an energy density analysis is necessary. As previously mentioned, the goal of using multiple energy sources is to fully leverage their unique characteristics. For instance, if a vehicle is intended for a shorter mission, it may be advantageous to exclude the fuel cell, which would otherwise remain underutilized, resulting in a reduction in overall weight. For this reason, it is possible to study the system under different configurations. Excluding the flywheel and assuming the electric motor and power electronics common to all systems the possible configurations are:

- **B**
- **B + SC**
- **FC + B**
- **FC + SC**
- **FC + B + SC**

These configurations offer varying levels of energy density, autonomy, response time and power. The choice of configuration can be made based on the specific characteristics needed for different routes and applications of WIG vehicles. For this study, the most complex configuration (FC + B + SC) will be analyzed, as it can be broken down into simpler subsystems representing other configurations.

## 2.2 Topology

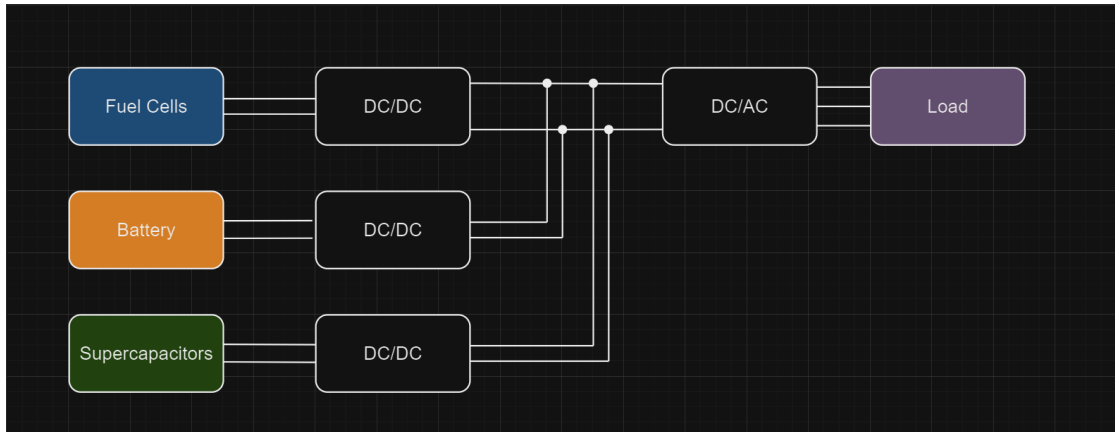
Once the configuration is chosen, the next step is to determine the optimal way to connect the components. Energy Management System (EMS) strategies control energy flow among the sources through converters. To maximize flexibility and fully leverage these strategies, the best topology would involve connecting each component, to a common bus, with a dedicated converter. However, it's important to consider that each converter introduces inefficiencies, adds weight, and increases costs. For this reason, a topology study is needed to balance the trade-offs between system flexibility, efficiency, weight and cost. This study will help identify the most suitable configuration, determining whether the benefits of using dedicated converters outweigh the drawbacks, or if shared or simplified converter arrangements can still meet the system's performance requirements. All the configurations studied have in common the DC/AC inverter that links the bus to the load. As topology of converter, it has been considered an unidirectional DC/DC converter for the Fuel Cells and a bidirectional DC/DC converter for both Battery and Supercapacitors. Several possibilities are studied in the succeeding subsections.

### 2.2.1 One unidirectional DC/DC converter for Fuel Cells and two bidirectional DC/DC converters for Battery and Supercapacitors

In this configuration (Figure 2.1a), each energy source is equipped with its own dedicated converter, allowing the EMS strategies to exercise precise control over the energy flow within the system. By assigning a dedicated converter to each component, the converters can be specifically tailored and optimized for the unique characteristics and requirements of the fuel cells, battery, and supercapacitor. This approach maximizes efficiency in managing energy transitions and enables the EMS to finely tune the system's performance.

However, incorporating three separate converters introduces significant drawbacks. The addition of multiple units increases overall system inefficiencies due to power conversion losses. It also adds considerable weight and cost, which can be a critical concern, especially in applications where space and weight are limited or highly constrained, such as in electric vehicles or aerospace systems.

Moreover, this topology significantly raises the complexity of the EMS. With three distinct components to manage, the EMS must handle multiple power sources, translating to a higher number of control signals, potentially up to ten different signals (Section 3.1). This not only increases the computational demand on the EMS but also requires more sophisticated algorithms to ensure optimal performance across the entire system. As a result, while this configuration offers flexibility and control, it also imposes additional challenges in terms of system complexity, cost and efficiency.



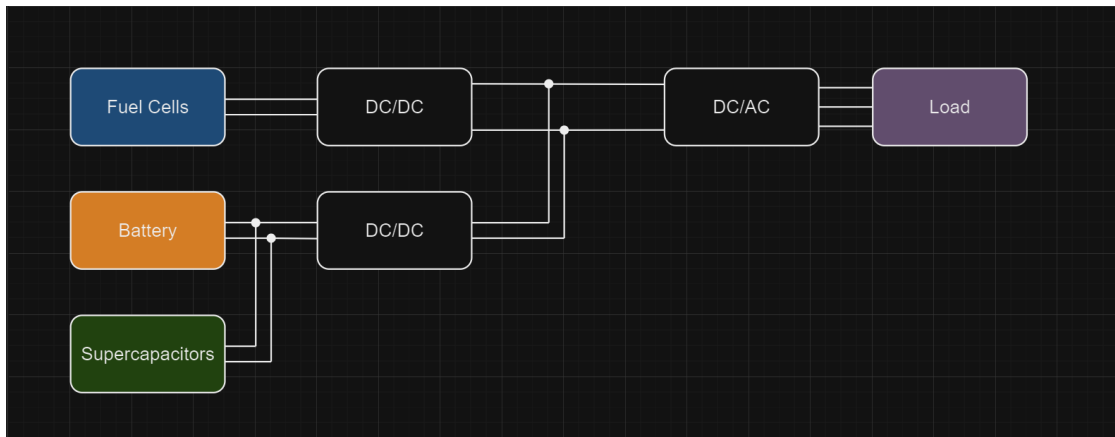
(a) 1 unidirectional DC/DC converter FC  
2 bidirectional DC/DC converters B+SC

**Figure 2.1:** Topology study schemes (a)

## 2.2.2 One unidirectional DC/DC converter for Fuel Cells and one bidirectional DC/DC converter for Battery and Supercapacitors

This configuration (Figure 2.1b), with respect to the first one, reduces the number of converters by using one to be shared between battery and supercapacitors making it lighter and cheaper. Moreover, the supercapacitor's fast response and battery's energy storage are complementary, making this combination efficient. Nevertheless control algorithms may become more complex to manage the hybrid battery-supercapacitor interface and potential voltage mismatch between battery and supercapacitor, requiring precise control.

A potential solution to some of these challenges is using a multi-input DC/DC converter[15]. This approach allows a single converter to manage two different energy sources by utilizing advanced control algorithms to regulate the power flow from each source. The control system can prioritize energy supply based on the system's needs, such as drawing from the supercapacitor for quick bursts of power and from the battery for sustained energy delivery. However, this configuration would still result in a complex control system, as the integrated converter must be designed to handle the unique characteristics of both energy sources.

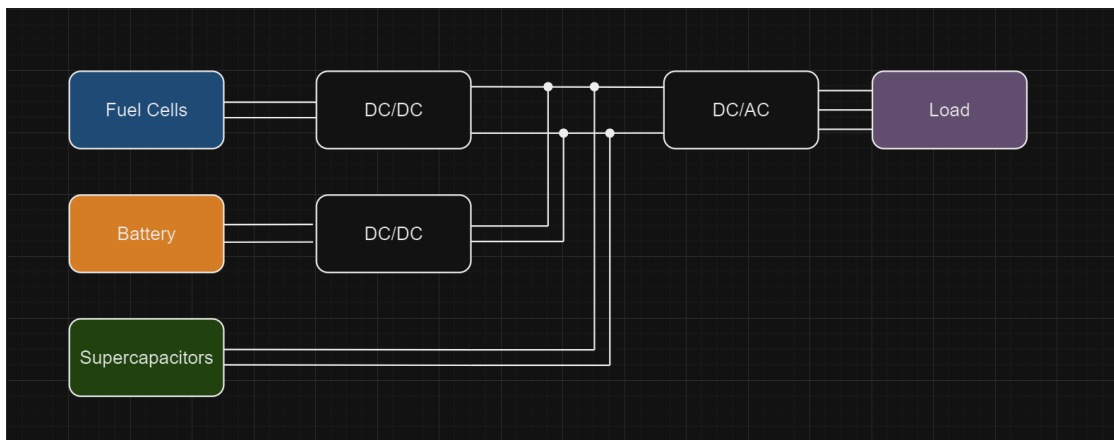


(b) 1 unidirectional DC/DC converter FC  
1 bidirectional DC/DC converter B+SC

**Figure 2.1:** Topology study schemes (b)

### 2.2.3 One unidirectional DC/DC converter for Fuel Cells and one bidirectional DC/DC converter for Battery

With one dedicated unidirectional DC/DC converter for the Fuel Cells and another one bidirectional for Battery (Figure 2.1c) the Supercapacitors are left connected passively to the DC bus. The system is simplified by eliminating one converter and supercapacitor naturally responds to power fluctuations, as its voltage fluctuates according to the state of the DC bus. However EMS has less control over the supercapacitor's power flow since it's passive and SC voltage will fluctuate based on the bus voltage, limiting its energy storage capacity utilization.

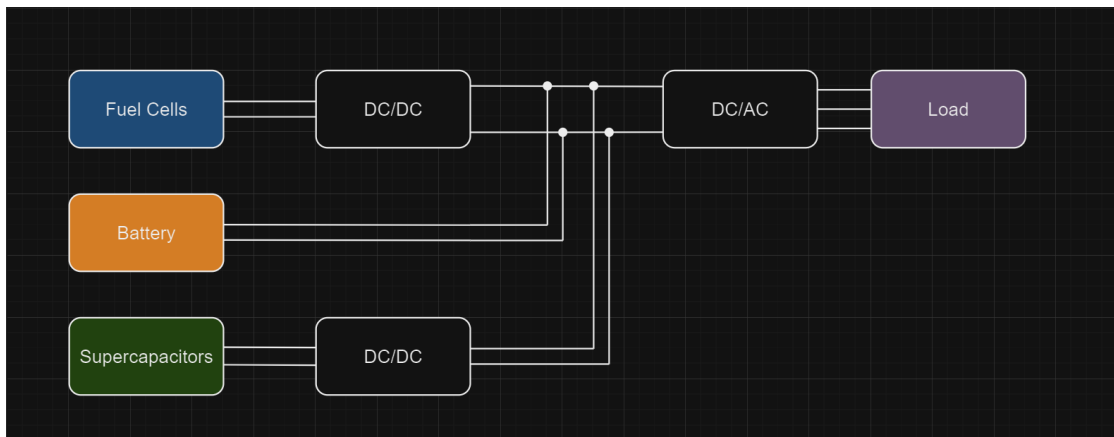


(c) 1 unidirectional DC/DC converter FC  
1 bidirectional DC/DC converter B

**Figure 2.1:** Topology study schemes (c)

### 2.2.4 One unidirectional DC/DC converter for Fuel Cells and two bidirectional DC/DC converter for Supercapacitors

A mirror topology (Figure 2.1d) to the one just described, it presents a bidirectional converter for the supercapacitors while leaving the battery directly connected to the bus. In this case, control of the battery is dispensed with by letting it directly support the bus, reducing conversion losses and improving efficiency during steady power demand. Nevertheless, the absence of a converter for the battery means less control over its power output and input, possibly making it harder to regulate voltage or protect the battery from overcharging/discharging. In fact, managing the voltage synchronization between the battery and the bus becomes crucial to prevent performance or safety issues.

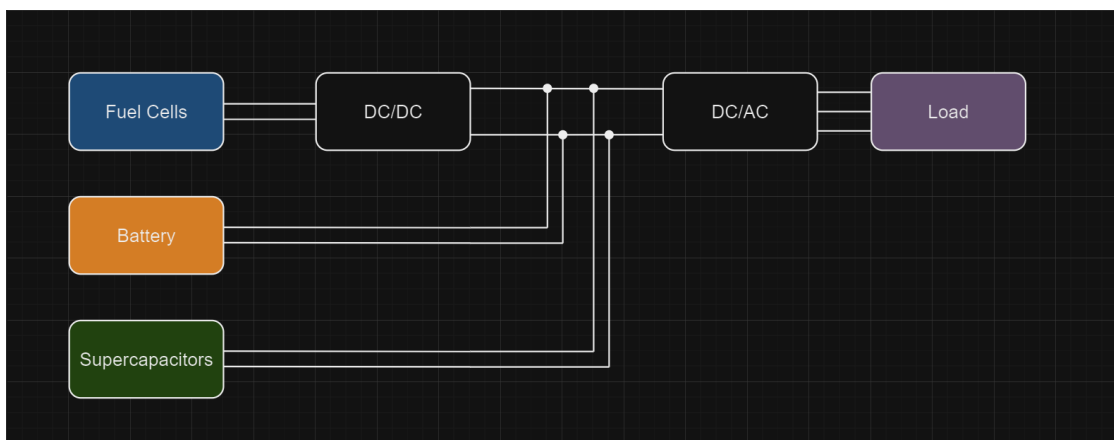


(d) 1 unidirectional DC/DC converter FC  
1 bidirectional DC/DC converter SC

**Figure 2.1:** Topology study schemes (d)

### 2.2.5 One unidirectional DC/DC converter for Fuel Cells

In this configuration (Figure 2.1e), only the fuel cell is connected to the system via a DC/DC converter, while the battery and supercapacitor are passively connected to the DC bus. This significantly simplifies the system by reducing the number of converters, which lowers costs, weight, and complexity. It also improves overall efficiency by avoiding conversion losses, especially during high-power demands or quick energy bursts. However, with this setup, the EMS has control only over the fuel cells, limiting flexibility in energy management, particularly during transitions. Additionally, regulating bus voltage becomes more challenging, as the direct connection of the battery and supercapacitor can introduce fluctuations.



(e) 1 unidirectional DC/DC converter FC

**Figure 2.1:** Topology study schemes (e)

The ones described are few of the potential possibilities to be studied. The next step would be implementing all of them in simulation and take a choice on the base of several parameters:

- Converter Count
- Reliability and Maintenance
- Efficiency
- Control complexity
- Flexibility
- Weight and Volume
- Cost

Taking into account that this procedure would require a lot of time, and since is not strictly necessary at this point of the study, the choice was taken on the base of the just discussed theoretical considerations.

The best compromise between pro and contra avoiding safety problems is the configuration with one unidirectional DC/DC converter for the fuel cells and one bidirectional DC/DC converter for the battery leaving the supercapacitors directly linked to the common bus.

## 2.3 System Sizing

In order to size the energy system components, it is essential to consider typical load demands, including average power, peak power, and response to transient loads. These features allow the computation of each component characteristics to better take advantage of the strengths of each one. Current progress in the project allows for using two scaled model for field tests, which has provided typical power consumption data during takeoff. More details on testing conditions and methodologies will be provided in Section 4.

Additionally, a mathematical approach, as outlined in "A Study on Estimation of Propulsive Power for Wing in Ground Effect (WIG) Craft to Take-off"[16], was used as a reference to understand the underlying physics, although it is more beneficial for fluid dynamic design than energy system design. Therefore, data from sensors during tests have been used for accurate sizing (Figure 4.3).

Starting from load characteristics (Table 2.1) and assuming a theoretical efficiency for the converter  $\eta = 80\%$ , the design approach follows the steps described in the subsequent paragraphs.

Characteristic	Symbol	Value
Average Power	$P_{mean}$	2.5 kW
Peak Power	$P_{peak}$	10 kW
Max Continuous Mode Power	$P_{max,cont}$	3 kW
Transient Peak Power	$P_{trans}$	10 kW
Pre-Rolling Power	$P_{pre-roll}$	2kW
Operational Time	$t_{op}$	630 s
Transient Time	$t_{trans}$	10 s

**Table 2.1:** Main characteristics of a scale model take-off typical load pattern

### 2.3.1 Fuel Cells

Fuel cells are a critical component of the power system for a WIG vehicle, providing a reliable and efficient source of energy to meet the average power demand during flight operations. Fuel cells operate by converting chemical energy from hydrogen into electrical energy through an electrochemical reaction, which produces water and heat as byproducts.

The fuel cell system, in the WIG vehicle, is designed to handle the average power requirement during the flight. This design ensures that the system operates optimally during steady-state conditions without being oversized, which could lead to unnecessary weight and inefficiencies. The nominal power of the fuel cell is determined based on the vehicle's mean power demand, denoted by  $P_{mean}$ , and the overall efficiency of the power conversion system  $\eta$ .

$$P_{fc,nominal} = P_{mean} \cdot \eta \quad (2.1)$$

Here,  $P_{fc,nominal}$  represents the nominal power output of the fuel cell. This nominal power is theoretical and serves as the baseline for system design. During the selection process, commercially available fuel cells must be evaluated to ensure they work around this power requirement point.

Additionally, while the nominal power output is designed for average conditions, the design process may also consider the maximum power output of the fuel cell. By taking the maximum output into account, the size of supplementary energy storage devices, such as the battery and supercapacitor, can be reduced. This approach allows the fuel cell to handle a greater portion of the peak power demands, reducing reliance on the battery and supercapacitor for high-load conditions. Consequently, this could lead to a more efficient and lightweight system, without compromising performance during peak power events.

### 2.3.2 Batteries

The battery pack plays a vital role in compensating for power shortfalls when the fuel cell output is insufficient to meet the peak power demand. During such instances, the battery delivers the necessary power to bridge the gap between the peak load and the average power provided by the fuel cell. This relationship can be expressed as:

$$P_{batt,max} = P_{peak} - P_{mean} \quad (2.2)$$

The battery must also have enough energy capacity to provide continuous support over the entire operational duration. This ensures that the battery can supply power whenever needed without depleting prematurely. The capacity required for this purpose is determined by the following equation:

$$C_{batt} = \frac{P_{max,cont} - P_{mean}}{\eta} \cdot t_{op} \quad (2.3)$$

In the context of energy storage for WIG vehicles, lithium-ion batteries have traditionally been considered the most suitable option due to their high energy density, relatively lightweight design, and favorable performance characteristics[17]. However, recent advancements in solid-state battery technology present a promising alternative. Solid-state batteries offer several potential advantages over conventional lithium-ion cells, including higher energy density, improved safety, and longer lifespans due to their use of solid electrolytes instead of liquid ones. As solid-state batteries continue to develop, they may become a key technology for future high-performance aviation systems, providing more energy in a lighter and safer package. The potential and future role of solid-state batteries will be discussed in more detail in Section 2.4.2.

Regardless of the battery technology selected, it is essential to preserve the health of the battery by avoiding deep discharges, which can degrade its capacity over time. This is controlled by a parameter known as the **Depth of Discharge (DOD)**, which defines the portion of the battery's total capacity that is actively utilized during operation. By limiting the DOD, the system ensures prolonged battery life and reliability. With the capacity calculated to meet operational demands, the total battery capacity, considering the DOD, can be expressed as:

$$C_{batt,tot} = \frac{C_{batt}}{DOD_{batt}} \quad (2.4)$$

By accounting for the DOD, the final battery sizing not only ensures the battery can handle power demands but also extends the lifespan of the energy storage system.

### 2.3.3 Supercapacitors

Supercapacitors are integrated into the power system to handle rapid power demands, particularly during transient conditions when there are sharp increases in power requirements. These devices are well-suited for applications where short bursts of high power are needed, due to their ability to charge and discharge quickly with minimal energy loss.

The power handled by the supercapacitor during these transient events can be expressed as:

$$P_{sc,max} = P_{trans} - P_{pre-roll} \quad (2.5)$$

Where  $P_{trans}$  represents the power required during the transient event, and  $P_{pre-roll}$  refers to the power required right before the takeoff phase, specifically when the WIG vehicle starts to move and slowly gains speed. During this phase, the vehicle is still overcoming the static hydrodynamic forces acting on its hull as it moves through water, but the power demand is relatively low. As the vehicle accelerates and transitions towards takeoff, the power requirements rise sharply, which is where the supercapacitors step in to provide the necessary boost.

The energy required from the supercapacitors is determined by the duration of the transient event  $t_{trans}$  and can be calculated as follows:

$$C_{sc} = P_{trans} \cdot t_{trans} \quad (2.6)$$

Similarly to batteries, the total capacity of the supercapacitor system must account for the fact that only a portion of the energy storage can be safely utilized to maintain long-term performance. This is controlled by the **Depth of Discharge (DOD)** parameter. The total supercapacitor capacity is therefore expressed as:

$$C_{sc,tot} = \frac{C_{sc}}{DOD_{sc}} \quad (2.7)$$

In high-performance applications, such as those involving dynamic vehicle operations with frequent power spikes, like military operations where quick response times and agility are paramount, the supercapacitors system might need to be scaled up to ensure sufficient energy storage and delivery. For now, a scale factor ( $\chi$ ) is applied to account for uncertainties in system design and to provide a margin for safety, as real-world operations may demand more power than anticipated during transient events. The scaled supercapacitor capacity is given by:

$$C_{sc,scal} = C_{sc,tot} \cdot \chi \quad (2.8)$$

This scaling ensures that the system remains robust enough to handle a wide range of operating conditions. However, the scaling factor can be specifically applied to vehicles commissioned for roles that demand rapid power responses, such as military or high-performance applications. For standard civilian or less-demanding roles, this oversizing approach can be avoided, allowing for more efficient designs without unnecessarily increasing the size and weight of the supercapacitor system when such performance margins are not required. However, once these type of maneuvers are conducted in field tests and the system's performance is validated under real-world conditions, the scaling factor ( $\chi$ ) may no longer be necessary. These tests will provide a clearer understanding of the power requirements during dynamic maneuvers, allowing for precise system optimization without the need for oversizing. This will result in a more efficient and lightweight design tailored to the actual demands of the application.

### 2.3.4 Power System Characteristics

The power system components are sized to meet the operational demands of the WIG vehicle, accounting for transient power requirements and sustained energy delivery. Considering a scale factor  $\chi = 1.3$  to provide a margin for safety and flexibility, and a Depth of Discharge (DOD) of 40% for both the battery and supercapacitors, the components chosen for the energy system must meet the following specifications:

Fuel Cells	continuous power	3.1 kW
Battery	max power capacity	9.4 kW 152 Wh
SuperCapacitors	max power capacity	8 kW 90.2 Wh

**Table 2.2:** Energy system requirements

As mentioned earlier, these parameters can be further adjusted depending on the specific operational requirements of the vehicle. For example, the fuel cell system could be sized not only based on the average power demand but also considering its maximum power output to reduce reliance on the battery and supercapacitors for high power bursts. This design flexibility allows for optimizing the system to match the vehicle's mission profile, whether prioritizing endurance, responsiveness or energy efficiency, without unnecessarily oversizing components for less-demanding scenarios.

## 2.4 Components

The following paragraphs introduce a preliminary investigation into the commercial market for components and latest technologies that match the requirements previously described.

### 2.4.1 Fuel Cells

The H-3000 Fuel Cells (Appendix B.1), part of the H-series and developed by Horizon Fuel Cell Technologies[18] fit the characteristics required for the energy system, moreover, they have been chosen, apart from their excellent performance, because of the amount of details provided by the company; in fact, this aspect is relevant to be able to run more accurate simulations with results closer to the reality.

## 2.4.2 Battery

As briefly mentioned above, at the current time, the most widespread and performing battery technology is lithium-ion. However, given the innovative nature of this study and the inclination toward new technologies, solid-state batteries are considered as the main solution (Appendix B.2).

Solid-state batteries (SSBs) are a promising next-generation technology for electric mobility, offering several advantages over traditional lithium-ion batteries (LiBs) used in electric vehicles (EVs) today. Solid-state batteries replace the liquid or gel electrolyte in conventional LiBs with a solid electrolyte, leading to several improvements:

- **Higher Energy Density:** Solid-state batteries can store more energy per unit of volume or weight compared to current LiBs. This increased energy density translates to longer driving ranges for electric vehicles without requiring a proportional increase in battery size.
- **Improved Safety:** Traditional lithium-ion batteries use liquid electrolytes, which can leak, catch fire, or explode under certain conditions (such as overheating or physical damage). Solid electrolytes are non-flammable, reducing the risk of thermal runaway, which enhances the overall safety of electric vehicles.
- **Faster Charging:** Solid-state batteries are expected to support faster charging rates compared to current lithium-ion batteries. Some SSB designs could potentially offer charging times comparable to filling a gas tank, which is critical for consumer adoption in the EV sector.
- **Longer Lifespan:** Solid-state batteries are more resistant to the formation of dendrites. By mitigating dendrite formation, SSBs could offer significantly longer lifespans, which is advantageous for electric vehicles requiring long-term durability.
- **Greater Temperature Tolerance:** Solid-state batteries can operate efficiently across a wider temperature range, making them suitable for a variety of climates. This characteristic is particularly important for e-mobility applications in regions with extreme weather conditions.

However, despite their potential SSBs still face significant challenges:

- **Cost:** Manufacturing solid-state batteries is currently more expensive than traditional lithium-ion batteries due to the complex processes involved and the relatively low scale of production.

- **Materials and Manufacturing:** The development of solid electrolytes that are both stable and scalable is still in progress. Many promising solid electrolyte materials, such as sulfides and oxides, are being researched, but each comes with its own set of manufacturing challenges, including brittleness, interfacial resistance and processing difficulty.
- **Durability and Cycling Stability:** While SSBs are believed to have longer lifespans, they are still in the early stages of development. Ensuring that these batteries can withstand thousands of charge and discharge cycles while maintaining performance is a key challenge that needs to be addressed.
- **Anode Development:** The use of lithium metal anodes is a major goal for solid-state batteries, as it can dramatically increase energy density. However, achieving stable, dendrite-free lithium metal anode operation with solid electrolytes has proven to be difficult, although advances are being made.

While many of the current drawbacks associated with solid-state batteries (SSBs) are tied to their early-stage development, ongoing research is addressing these challenges, particularly when it comes to anode materials. One promising area of research is the use of silicon nanowires[19]. Silicon has a significantly higher theoretical capacity compared to traditional graphite anodes. However, bulk silicon faces issues with volume expansion during lithiation (charging), which can lead to mechanical degradation. Using silicon in the form of nanowires helps to mitigate this problem. The nanowire structure allows for more flexible accommodation of volume changes, additionally, silicon nanowires provide a high surface area and ensure more uniform interaction with the solid electrolyte, which can lower interfacial resistance and improve the efficiency of lithium-ion transport. These properties not only enhance the performance of the battery but also contribute to its long-term stability. As a result, silicon nanowires are emerging as a viable alternative to traditional anodes while lithium metal anode technology continues to develop.

### 2.4.3 Supercapacitors

Supercapacitors play a critical role in the energy system of a WIG (Wing in Ground Effect) vehicle due to the unique demands placed on these vehicles. In emergency or high-stakes situations, such as the need for rapid acceleration or evasive maneuvers, the energy system must be capable of delivering power instantaneously. Supercapacitors are particularly well-suited for this purpose due to their ability to rapidly discharge large amounts of energy, making them ideal for handling short, high-power bursts that batteries and fuel cells alone may struggle to meet.

For this application, the Skeleton SkelCap technology has been identified as a suitable, in particular, the SCX5000 cell. This model is designed with advanced ultracapacitor technology, offering a combination of high power density and low equivalent series resistance (ESR), which is crucial for fast power delivery. The individual cell SCX5000 is capable of delivering 3V with a rated capacitance of 5000 farads (F) and an impressively low ESR of just 0.14 milliohms ( $m\Omega$ ). This low internal resistance enables it to provide high efficiency during both charge and discharge cycles, ensuring minimal energy losses.

Additionally, the robust performance of this supercapacitor makes it particularly valuable in scenarios where frequent power cycling is required, as it is highly durable and can undergo a large number of charge-discharge cycles without significant degradation. This characteristic enhances the overall reliability of the WIG vehicle's power system.

The performance and specifications of the Skeleton SCX5000, detailed in the Appendix B.3, demonstrate its suitability not just for civilian applications, but also for high-performance or military WIG vehicles, where agility and rapid energy deployment are essential.

## Chapter 3

# Energy Management System Strategies

After determining the configuration of components and selecting the appropriate power electronics topology, the next critical step involves optimizing their performance and interaction. This is achieved through the implementation of Energy Management System (EMS) strategies, which are designed to enhance system efficiency, balance power distribution and ensure smooth coordination between components under varying operating conditions.

### 3.1 General Working Principle

All EMS strategies, though varying in their specific approaches, share the common goal of leveraging the unique characteristics of each energy source through control signals. In this case, the selected topology includes one unidirectional DC/DC converter for the fuel cells and one bidirectional DC/DC converter for the battery (Figure 2.1c). Each converter controls energy flow using two signals:

- Output voltage
- Input current limitation

Since the battery's converter is bidirectional, a total of six signals is required. These signals make up the output of the Energy Management System, enabling efficient power flow control and system coordination.

The control of the common bus voltage ( $V_{dc,bus}$ ) is managed through the battery converters and apart from the External Energy Maximization Strategy (Section 3.2.6), remains consistent across all strategies. This control is achieved using a simple PI controller (Figure 3.1), which adjusts the system based on the difference

between the measured bus voltage ( $V_{dc,bus}$ ) and the desired reference voltage ( $V_{dc,ref}$ ). The key distinction between the strategies lies in how they compute the reference power for the fuel cells.

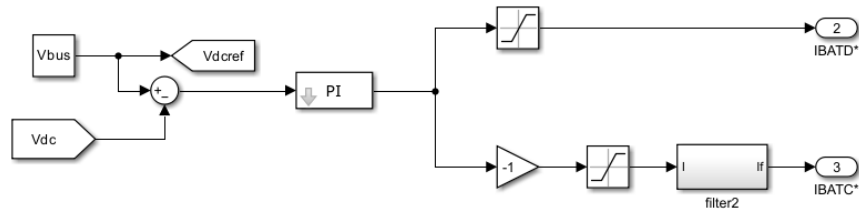


**Figure 3.1:** Battery converters control scheme

Once  $P_{fc}$  is computed using the different approaches, the converter efficiency and fuel cell voltage are considered to calculate the control signal, represented by the required current. Before delivering this signal to the fuel cell, as it is possible to notice in Figure 3.2, a check on the bus voltage  $V_{dc}$  is performed to ensure it stays within safe limits, as the common bus voltage cannot be too low or too high for safety reasons. If necessary, the current is adjusted accordingly to maintain proper operation.

## 3.2 Strategies Description

The strategy used to simulate the energy system and obtain different features are some of the most common:

- **State Machine Control Strategy**
- **Classical PI Control Strategy**
- **Rule Based Fuzzy Logic Control Strategy**
- **Frequency Decoupling and State Machine Control Strategy**
- **Equivalent Consumption Minimization Strategy (ECMS)**
- **External Energy Maximization Strategy (EEMS)**

Some of these strategies, also proposed by Souleman Njoya Motapon in "Design and simulation of a fuel cell hybrid emergency power system for a more electric aircraft: evaluation of energy management schemes"[7], have undergone modifications to address certain shortcomings identified during testing. As a result, a new strategy has been introduced:

- **Memory-Based Hysteresis PI Control(MH-PI)**

This new approach is based on the Classical PI Control and will be detailed in the next section (Section 3.3).

### 3.2.1 State Machine Control Strategy

The State Machine Control Strategy relies on predefined operating states to manage system behavior based on current conditions. Transitions between states are triggered by specific thresholds or events, that in this case are fixed as changes in battery state of charge (SOC) and power demand. This approach provides a simple and clear framework for managing power distribution by following well-defined rules. In particular, the rules define 8 different states as shown in Table 3.1

The state of the State of Charge (SOC) can be classified as "High", "Normal" or "Low", based on a defined range with two boundaries. Proper tuning of this range is crucial, as it can lead to different performance. Other values, such as  $P_{fc,min}$ ,  $P_{fc,max}$  and  $P_{fc,opt}$  are derived from component specifications. These values can be slightly adjusted depending on whether one prefers to prioritize safety or optimize component usage.

For example, in State 7, it is important to note that this is activated when the SOC is "Low" and the load power ( $P_{load}$ ) is less than  $P_{fc,max}$ . The action taken

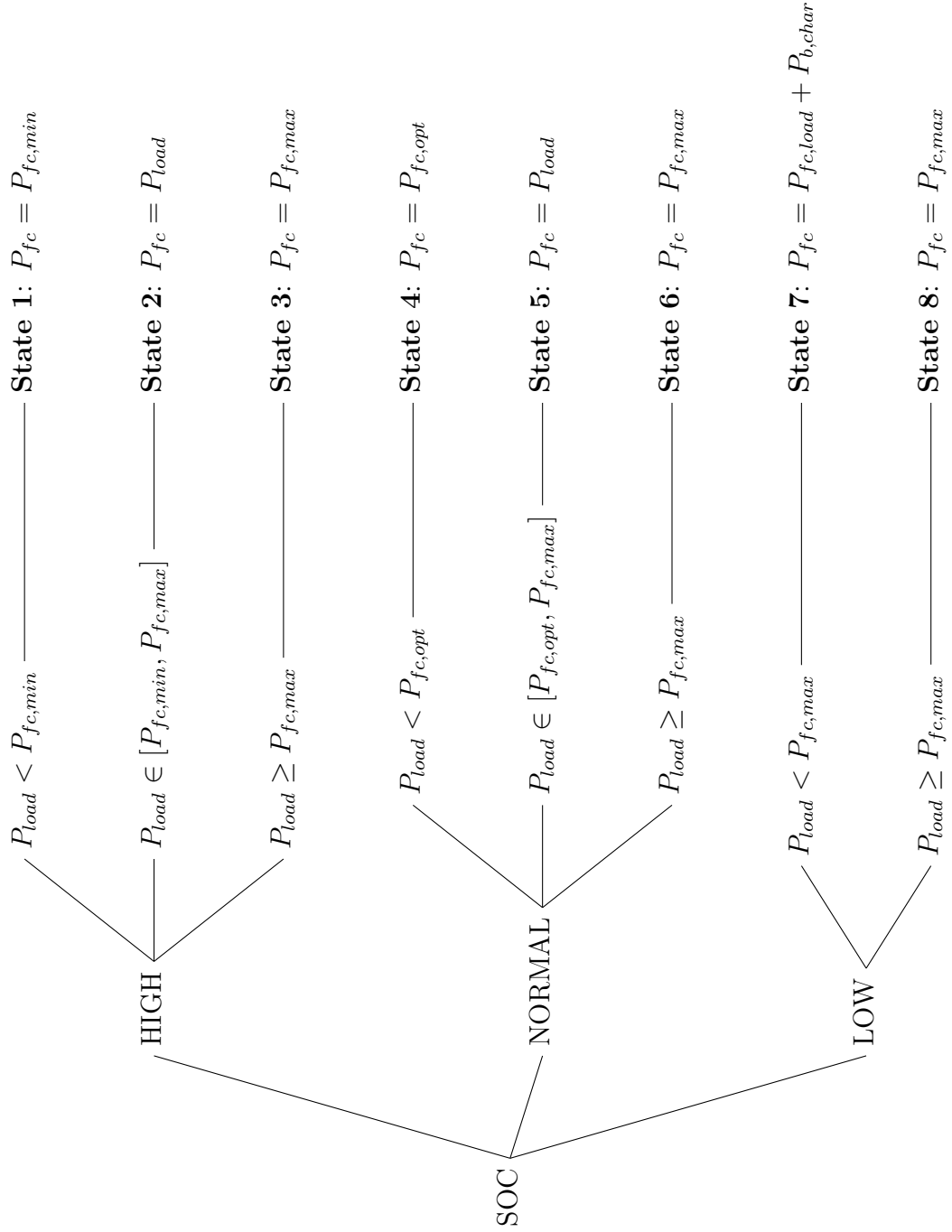


**Table 3.1:** State Machine Control: rule-based state transition diagram

in this scenario is to set the fuel cell output power equal to the sum of  $P_{load}$  and  $P_{b, char}$ . This implies that if  $P_{load}$  is marginally below  $P_{fc, max}$ , adding the fixed  $P_{b, char}$  value could result in a fuel cell power requirement that exceeds  $P_{fc, max}$ . Further improvement in this case is suggested as also simple solutions can be adopted to address this problem. Few examples could be:

- **Dynamic Adjustment of Charging Power:** Instead of having a fixed value, consider implementing a dynamic adjustment based on the current SOC and  $P_{load}$ .
- **Maximum Output Power Guaranteed:** Considering  $P_{fc}$  as the minimum between  $P_{load} + P_{b, char}$  and  $P_{fc, max}$

### 3.2.2 Classical PI Control Strategy

The Classical Proportional-Integral (PI) Control Strategy is a widely used feedback control mechanism. In the context of energy management, the PI controller continuously adjusts system parameters, such as power output, based on the error between a measured variable (SOC) and a desired setpoint.

While the Classical PI Control Strategy is simple to implement and effective in many steady-state conditions, it can struggle with dynamic or rapidly changing systems.

In this Energy Management System, the state of charge (SOC) of the battery is constantly monitored and compared to a predefined threshold (Figure 3.2). When the SOC exceeds the threshold, the control strategy directs the system to deliver maximum battery power, allowing full discharging to meet the load demand and let the Fuel Cells work efficiently. Conversely, when the SOC drops below the threshold, the system shifts to a recharging mode, restricting power delivery and focusing on replenishing the battery. This approach avoids the need for continuous modulation and feedback, providing a simpler yet effective way to manage energy flows by operating in distinct, binary states:

- maximum battery power output when the SOC is high
- battery recharging when the SOC is low

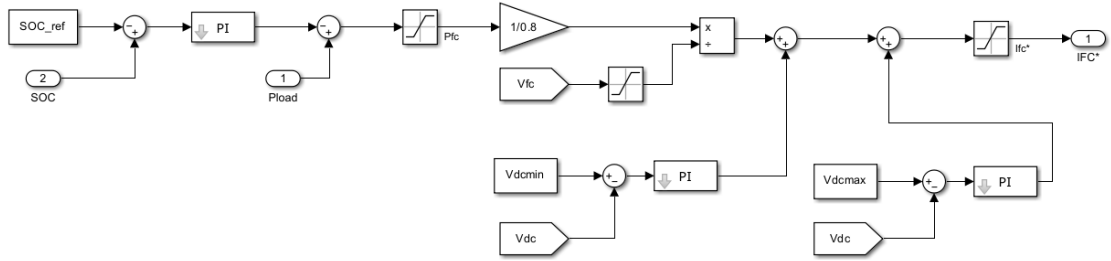


**Figure 3.2:** Classical PI Simulink scheme

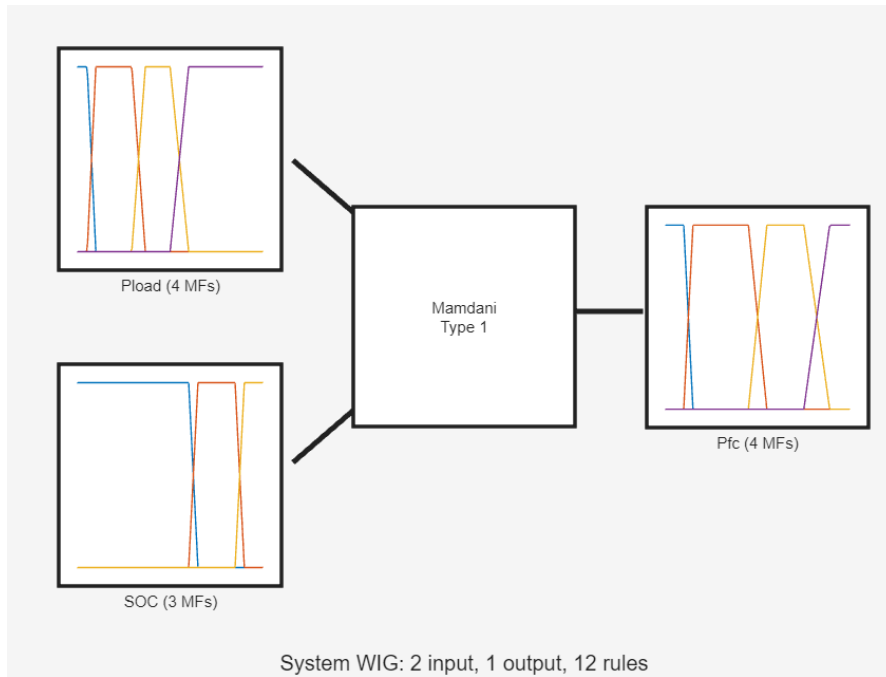
However, this type of controller can introduce fluctuations during steady-state operation, which is especially significant in the cruise mode of a Wing-In-Ground (WIG) vehicle (Figure 6.3). These fluctuations have negative impacts on several aspects, including overall performance, energy efficiency and the lifespan of system components. As these consequences are unacceptable, a new solution (Memory-Based Hysteresis PI Control, Section 3.3) was implemented to retain the advantages of the Classical PI control while eliminating the fluctuations.

### 3.2.3 Rule Based Fuzzy Logic Control Strategy

The Rule-Based Fuzzy Logic Control Strategy takes a more flexible approach compared to traditional control methods like PI. Fuzzy logic controllers are particularly effective in systems where the relationships between inputs and outputs are too complex or nonlinear for conventional controllers. Instead of relying on precise input values and thresholds, fuzzy logic uses linguistic variables (e.g., “low,” “medium,” “high”) and a set of heuristic if-then rules to manage system behavior. For this application the same set of 8 if-then rules used for the State Machine Control Strategy (Table 3.1) have been used (Figure 3.3e).

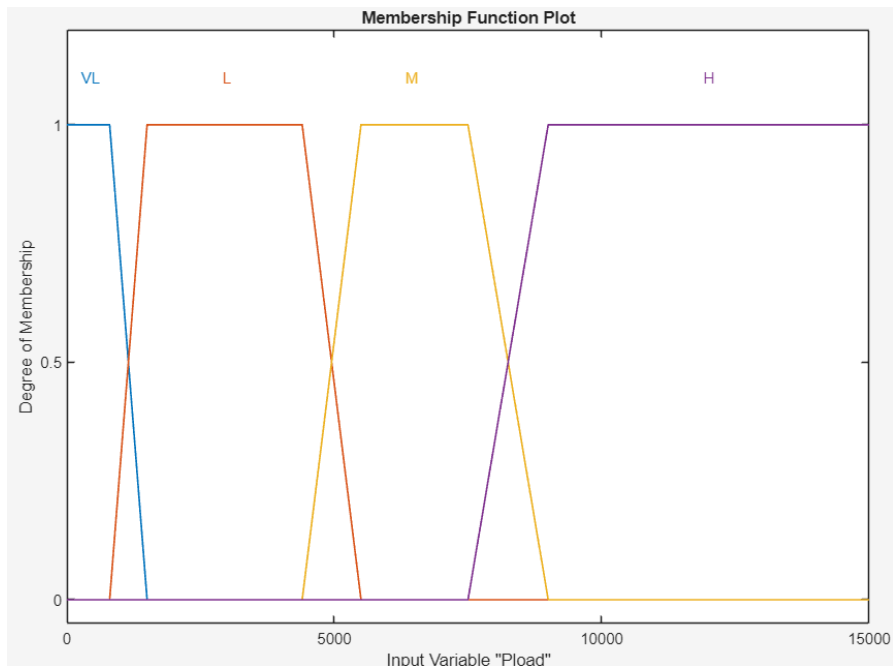
In energy management systems, fuzzy logic proves valuable for handling uncertainties, such as fluctuating power demands or unpredictable energy production from renewable sources. In this case, the controller takes the battery state of charge (SOC) and power load ( $P_{load}$ ) as input variables, converting them into fuzzy sets. It then applies the set of the 8 rules to determine the appropriate control action. This is achieved using the Mamdani-type 1 approach, one of the most widely used fuzzy inference systems. Finally, the control action is obtained through the Centroid Method used to defuzzify the fuzzy sets into crisp values for practical implementation.

The rules were constructed using the Fuzzy Logic Toolbox in MATLAB (Figure 3.3), which provided a valuable tool for fine-tuning the rules in a more intuitive and user-friendly manner.



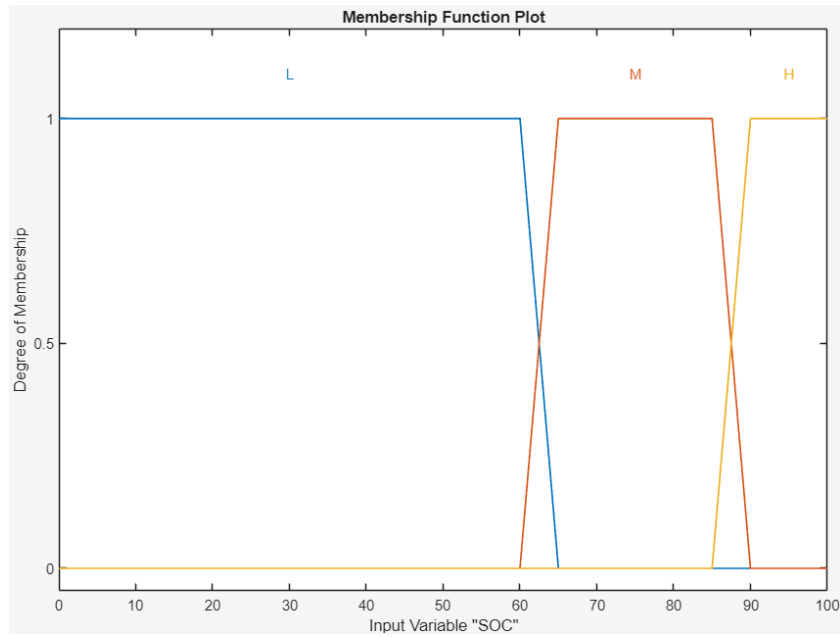
(a) Fuzzy Inference System (FIS) Plot

**Figure 3.3:** Matlab Toolbox - Fuzzy Logic Designer (a)



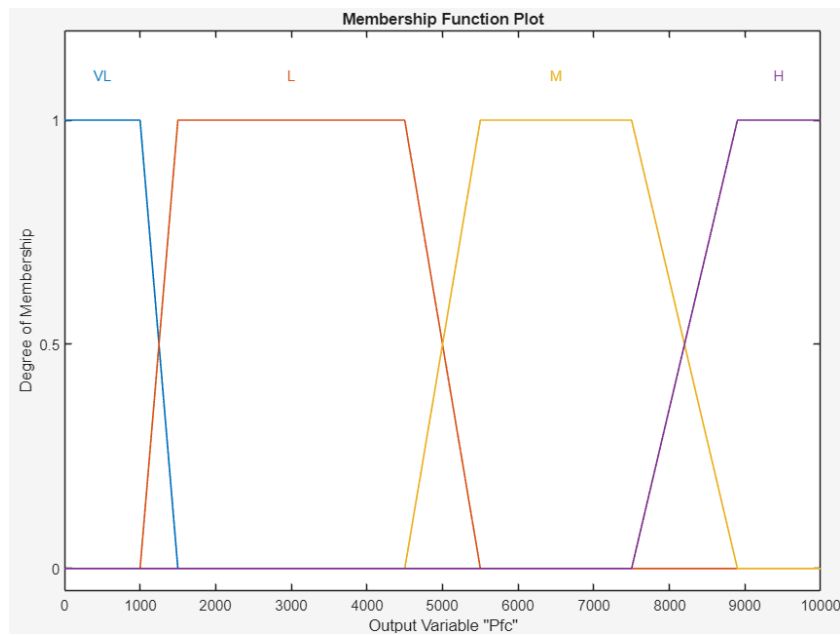
(b)  $P_{load}$  Membership Function

**Figure 3.3:** Matlab Toolbox - Fuzzy Logic Designer (b)



(c) SOC Membership Function

Figure 3.3: Matlab Toolbox - Fuzzy Logic Designer (c)



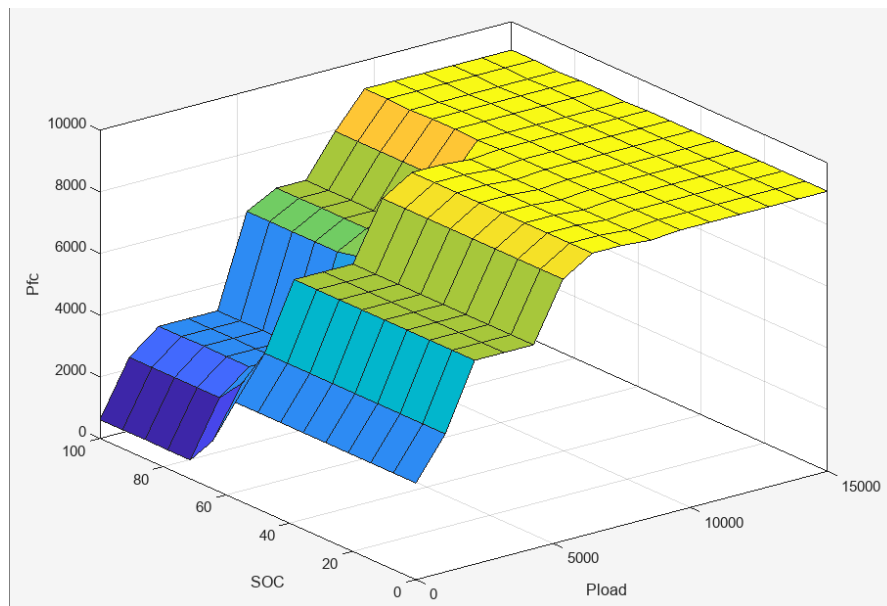
(d)  $P_{fc}$  Membership Function

Figure 3.3: Matlab Toolbox - Fuzzy Logic Designer (d)

	Rule	Weight	Name
1	If Pload is VL and SOC is H then Pfc is VL	1	rule1
2	If Pload is L and SOC is H then Pfc is L	1	rule2
3	If Pload is M and SOC is H then Pfc is M	1	rule3
4	If Pload is H and SOC is H then Pfc is H	1	rule4
5	If Pload is VL and SOC is M then Pfc is VL	1	rule5
6	If Pload is L and SOC is M then Pfc is L	1	rule6
7	If Pload is M and SOC is M then Pfc is M	1	rule7
8	If Pload is H and SOC is M then Pfc is H	1	rule8
9	If Pload is VL and SOC is L then Pfc is L	1	rule9
10	If Pload is L and SOC is L then Pfc is M	1	rule10
11	If Pload is M and SOC is L then Pfc is H	1	rule11
12	If Pload is H and SOC is L then Pfc is H	1	rule12

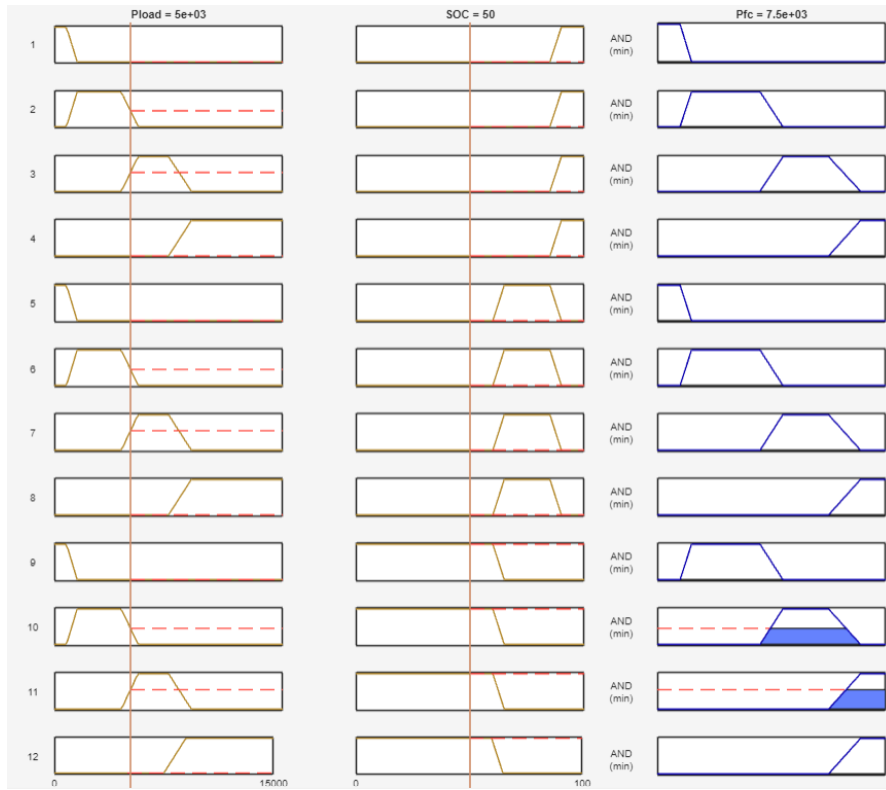
(e) Set of if-the Rules

Figure 3.3: Matlab Toolbox - Fuzzy Logic Designer (e)



(f) Fuzzy Control Surface

Figure 3.3: Matlab Toolbox - Fuzzy Logic Designer (f)



(g) Fuzzy Rules Inference

Figure 3.3: Matlab Toolbox - Fuzzy Logic Designer (g)

### 3.2.4 Frequency Decoupling and State Machine Control Strategy

The Frequency Decoupling and State Machine Control Strategy combines two complementary techniques to enhance energy management. The state machine framework governs high-level decision-making by switching between operating states (e.g. charging or discharging), while frequency decoupling separates the power demands into high and low-frequency components. This decoupling allows the system to assign different energy sources to different types of loads:

- **High-Frequency Loads:** such as transient power spikes, are typically handled by batteries or supercapacitors.
- **Low-Frequency Loads:** such as steady-state loads are managed by fuel cells.

Frequency decoupling was implemented using a low-pass filter, where the cutoff frequency can be adjusted to ensure the fuel cells provide nearly constant power. The State Machine control remains the same as described in Section 3.2.1, with the only difference being that the input signal is now filtered to remove the high-frequency component.

### 3.2.5 Equivalent Consumption Minimization Strategy

The Equivalent Consumption Minimization Strategy (ECMS)[20][7] is an advanced, real-time optimization method designed to reduce fuel consumption in hybrid power systems. ECMS treats both electrical energy stored in the battery and fuel consumed by fuel cell as equivalent in terms of energy consumption. The goal is to balance the energy use between these two sources in a way that minimizes overall fuel consumption. ECMS operates by continuously calculating the equivalent fuel consumption of using electrical energy (from the battery) and comparing it to the fuel consumption of directly powering the engine or generator. By dynamically shifting the load between the battery and the fuel-based power source, ECMS ensures that the system operates as efficiently as possible. This strategy is particularly beneficial for systems with fluctuating power demands, such as hybrid vehicles or grid-connected renewable energy systems, where it can optimize the use of stored energy to reduce fuel usage over time.

### 3.2.6 External Energy Maximization Strategy

The External Energy Maximization Strategy (EEMS)[7] is designed to prioritize the use of external energy sources such as solar energy over internal energy storage and prioritize the efficiency fuel-based power. The primary goal of EEMS is to maximize the utilization of these external resources to minimize fuel consumption.

In this case, the external energy sources are the battery and supercapacitors. The system monitors the availability of these two sources, ensuring they operate within their limits, while maximizing their usage to conserve the fuel cell's fuel. The EEMS is particularly beneficial in hybrid systems integrated with renewable energy sources, as it optimizes the balance between renewable generation, battery storage, and fuel consumption. As a proposed future enhancement, the integration of solar panels would further increase external energy utilization. By maximizing the use of external energy, EEMS not only improves fuel efficiency but also reduces operating costs and minimizes environmental impact.

### 3.3 Memory-Based Hysteresis PI Control Strategy

The Memory-Based Hysteresis PI Control (MH-PI) was developed to address the shortcomings of the Classical PI Control Strategy, particularly its steady-state fluctuations (Figure 6.3), which lead to safety risks and accentuate the wear and tear of components by decreasing their lifecycles.

The MH-PI strategy introduces a novel control mechanism that not only considers the battery's state of charge (SOC) but also takes into account its previous states and direction of change. This is achieved by defining two thresholds, creating three distinct regions within the SOC range:

- **Above Upper Range Limit:** When the SOC is above a specified upper limit, the system commands maximum battery power output. As result, the Fuel Cells power ( $P_{fc}$ ) is adjusted to meet the remaining load demand.
- **Within Range Limits:** When the SOC is within the defined thresholds, the control behavior depends on the history of the SOC. If the SOC is decreasing, the system continues to draw power from the battery; if it is increasing, the system switches to recharging mode. Specifically, the control adheres to the previous state, meaning the system retains the behavior from the last region it was in. Even if the SOC trend changes within the range, the control action is determined by whether the SOC was previously above or below the range. However, this scenario is unlikely, as a downward trend typically leads the battery to continue discharging, and an upward trend leads it to keep charging.
- **Below Lower Range Limit:** When the SOC is below a specified lower limit, the system commands the battery to recharge, requesting additional power from the fuel Cells.

By utilizing this approach, when the WIG vehicle enters cruise mode, representing a steady-state condition for the energy system, the battery is no longer required

to continuously charge and discharge around the reference SOC value. Instead, the system is stabilized, and fluctuations are minimized even within a narrow SOC range of just 2%. This adjustment effectively removes the cyclic fluctuations that would otherwise occur. Figure 3.4 illustrates the principle of operation for both the Classical PI and Memory-Based Hysteresis PI strategies, highlighting the key differences in their control logic.

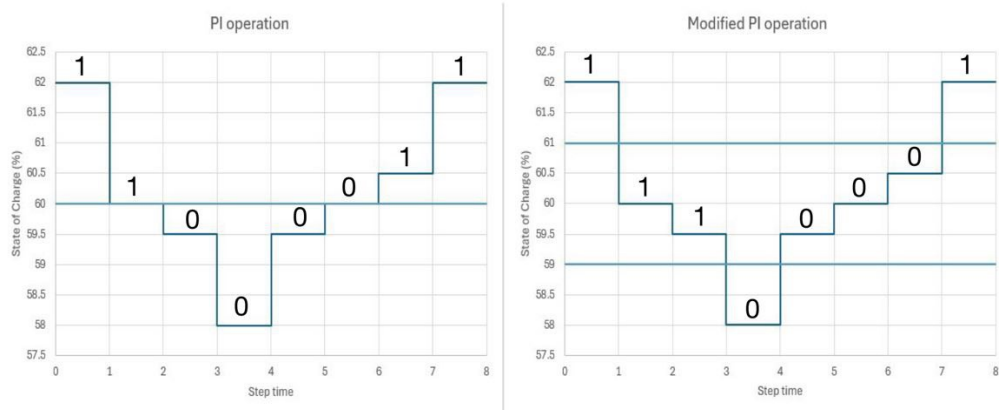


**Figure 3.4:** Operation Scheme - Classical PI (left) / Modified PI (right)  
**1:** Battery delivers its Max Power while from Fuel Cells is required the Power to meet the Load  
**0:** Fuel Cells deliver the Power necessary to satisfy the load requirement and to recharge the Battery

In the simulation environment, as shown in Figure 3.5, both PI strategies are implemented within the same subsystem, allowing for easy selection between them using a manual switch. This setup facilitates comparative analysis and helps identify the optimal strategy for different operational scenarios.

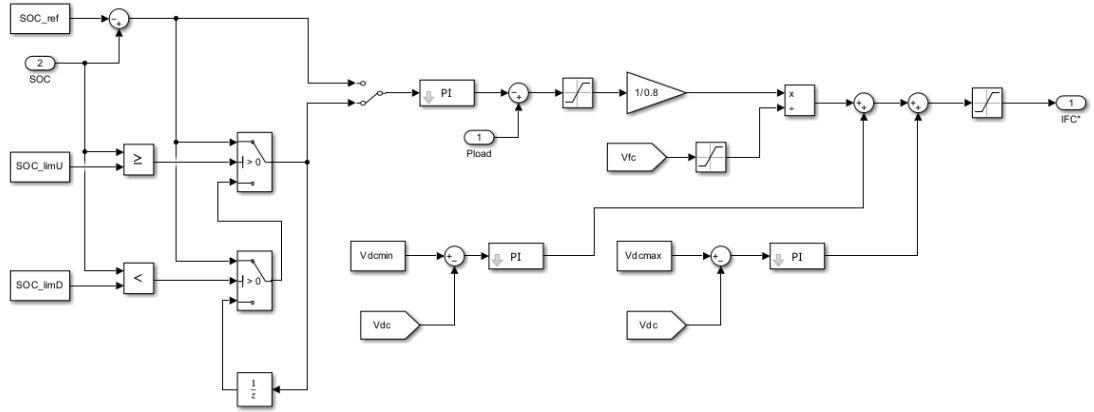


**Figure 3.5:** PI control scheme

One potential improvement to the Memory-Based Hysteresis PI Control (MH-PI) strategy is to dynamically adjust the two thresholds that define the SOC range during real-time operation. Instead of using fixed upper and lower limits, the system could continuously monitor factors such as power demand, fuel cells performance, battery health, and environmental conditions (e.g., temperature) to adaptively update these thresholds. This would allow the control strategy to respond more flexibly to changing conditions, optimizing power distribution and extending component lifecycles. For example, during periods of high power demand, the thresholds could be adjusted to prioritize battery discharge, helping to supplement fuel cell output and maintain system stability. Conversely, during lower demand or favorable conditions, the thresholds could be shifted to encourage battery recharging, by working with fuel cells at optimal power ( $P_{fc,opt}$ ) preserving fuel for later use. By dynamically updating the thresholds, the system could further improve efficiency, better balance the energy sources, and reduce the risks associated with SOC fluctuations.

## Chapter 4

# Typical Take-off Load Pattern

The current advancement of the project has enabled field tests using two different scale models:

- **Mistral** 1.5 meters wingspan (Figure 4.1)
- **Albatros** 2 meters wingspan (Figure 4.2)



**Figure 4.1:** Mistral - 1.5m wingspan scale model



**Figure 4.2:** Albatros - 2m wingspan scale model

Both models feature a reverse delta wing configuration and are powered by electric propulsion using batteries (for more details, refer to Appendix A).

The main objectives of the field tests were:

- **Behavior analysis:** Studying the models' performance both on water and in the air.
- **Power demand data:** Extracting power consumption patterns.

In terms of behavior, field tests facilitated adjustments to the hull shape to improve both hydrodynamic and aerodynamic efficiency. In terms of power demand, the tests not only provided data for the specific model but also revealed a typical take-off load pattern when comparing results from the different tests. This load pattern is characterized by the following phases (Figure 4.3):

- **Initial Acceleration Phase:** The power request starts at a lower level and gradually increases as the vehicle accelerates. This phase is crucial for overcoming the drag and inertia associated with the initial movement from a stationary position on water.
- **Peak Power Demand:** After the initial acceleration, the power demand rapidly rises, reaching a peak that is approximately five times the steady-state power required for cruising. This peak power is necessary to achieve sufficient speed for the wing to generate lift and transition from the water surface to the air.
- **Stabilization at Cruise Power:** Once airborne, the power demand decreases and stabilizes around a level that corresponds to the steady-state cruising speed of the vehicle. This lower power requirement is maintained during the cruise phase, as the lift generated by the wing reduces the drag and power needed.

Currently, flight stability has not yet been achieved with these models, which is why only the take-off maneuver has been tested. However, the takeoff load pattern, characterized by a rapid increase to a high peak power followed by a stabilization at cruising power, is highly demanding on the power system. This scenario can be considered one of the most strenuous maneuvers for a WIG vehicle due to the quick surge in power demand over a short period. Such a pattern is not only relevant for takeoff but also for other agile air maneuvers that might require similar power dynamics. For this reason, it was chosen as the focus for simulations.

The scalability of the load pattern allows the same principles to be applied to larger models or even full-scale Wing-in-Ground (WIG) vehicles. This ensures that the energy management strategies and key power components are selected appropriately across different vehicle sizes.

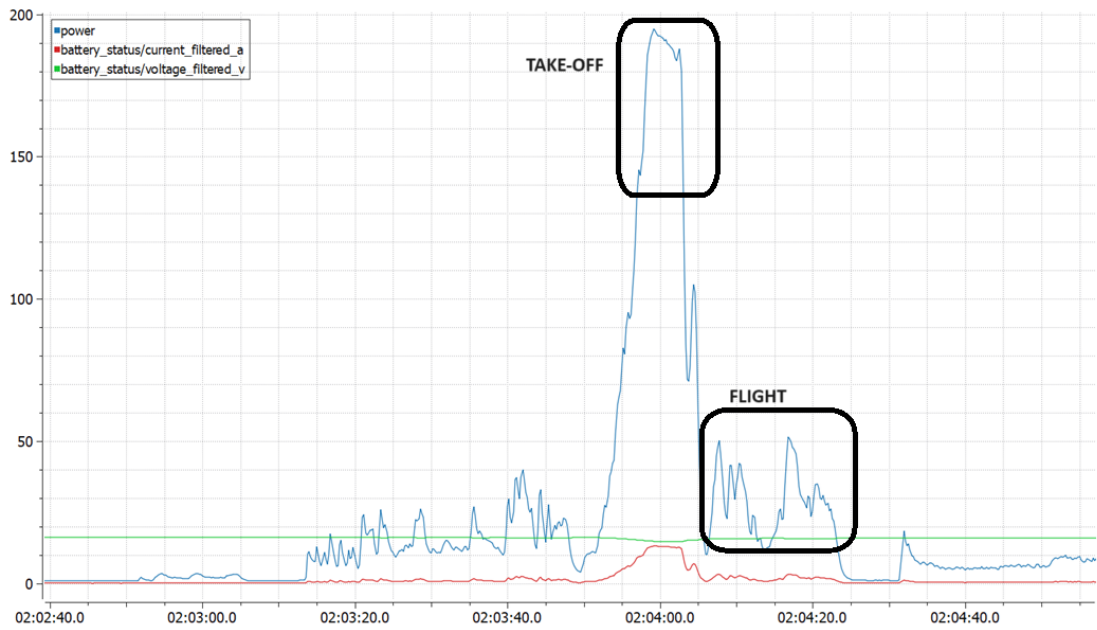


**Figure 4.3:** Field test data - Power Demand (Blue) / Current (Red) / Voltage (Green)

By applying these findings, it is possible to optimize energy systems for larger WIG craft, ensuring efficient power requirements for phases like take-off and cruising. Moreover, simulating the behavior of larger WIG vehicles before using real components offers a cost-effective way to test and refine the design, saving resources by avoiding direct full-scale testing initially.

# Chapter 5

## Simulation Details

The "Energy Management Systems for a Hybrid Electric Source"[21] Matlab (SimScape Power Systems) example was used as starting point simulation. The simulation (Figure 5.1) is an energy system proposed by S. N. Motapon [7] as solution for an emergency power system for a More Electric Aircraft (MEA). The system is composed by:

- Fuel Cells: nominal power 10kW
- Battery: 4 x 12.8 V, 40 Ah, Li-ion series connected modules
- Supercapacitors: 6 x 48.6 V, 88 F series connected modules

The initial simulation, which was originally designed to test the six strategies, encountered a number of issues. Notably, only the Frequency Decoupling Strategy, along with the Classical PI Control Strategy, were functioning as intended. This limited functionality hindered a comprehensive evaluation of all six strategies.

To address these issues, the first step involved identifying the root causes of the malfunctions in the remaining strategies. This process led to the development and implementation of new subsystems and f-functions specifically tailored to each strategy. Once the additional strategies were successfully integrated, a series of broader modifications were applied across the entire model.

This chapter outlines the key adjustments made to that model.

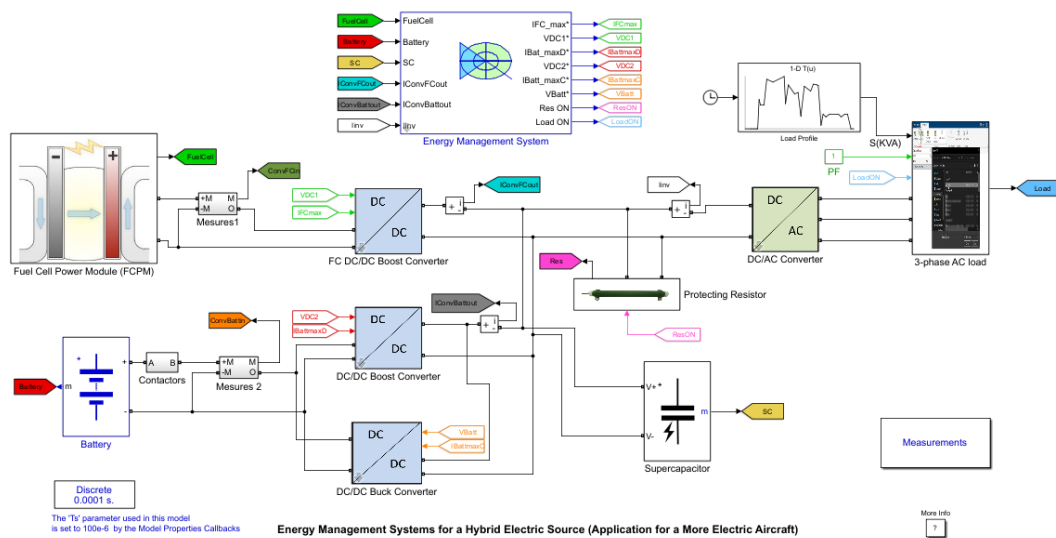
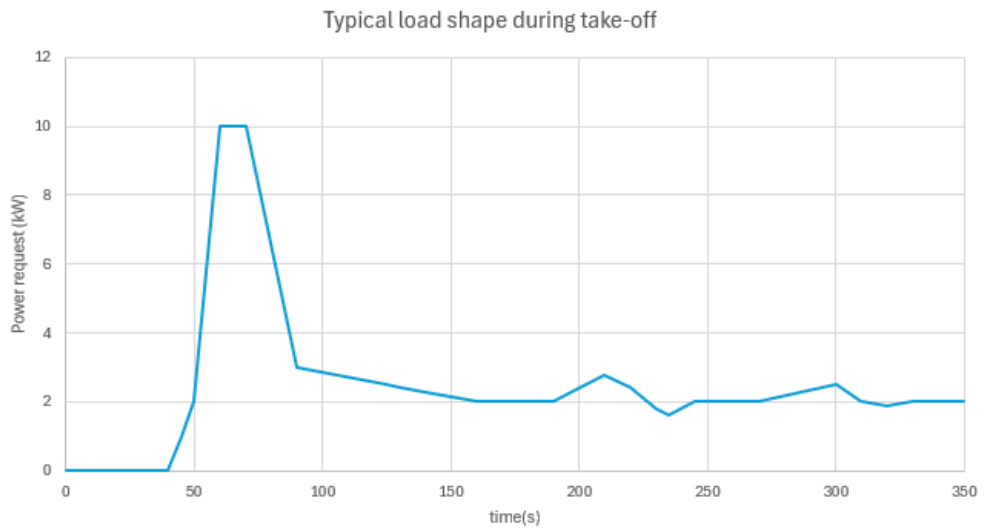


Figure 5.1: Original simulation

## 5.1 Load

Starting from the real data extracted from field tests (Figure 4.3) a "filtered" version of the pattern was created and rescaled to fit a third scale model of 5 meters wingspan (Figure 5.2). Specifically, this scaled model was tested on ice, a peak power of 10 kW during takeoff was determined. Given the typical takeoff pattern of WIG vehicles, the following curve was developed to evaluate the system and the proposed strategies:



**Figure 5.2:** Typical take-Off load pattern - filtered

The simulation utilizes a 3-phase AC load, provided by the mission profile through a look-up table. To simulate the system, a load profile lasting approximately 10 minutes was initially developed. However, due to the consistent runtime of each simulation, a shorter, more time-efficient load profile of about 5 minutes was implemented for the design phase and to monitor parameter changes step-by-step.

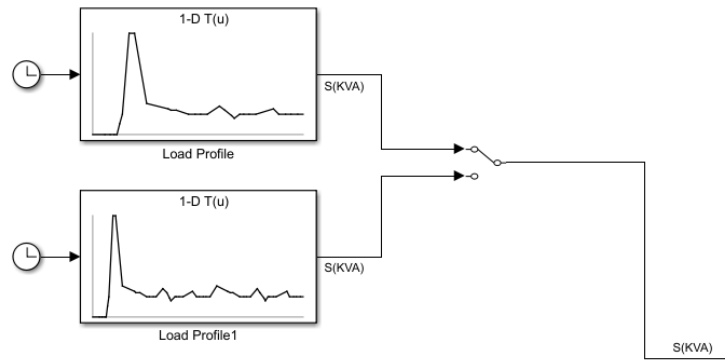


**Figure 5.3:** Lookup tables load profile - 5 mins(up) / 10 mins (down)

## 5.2 Parameters Setting

In the original version of the simulation, all components were fixed, and since their characteristics were put as numbers in each single block, it was not easy to modify the parameters that define those components. Due to the high complexity and the large number of parameters that needed to be adjusted across multiple blocks, a single Matlab function (Figure 5.4) was implemented to create useful variables. This user-friendly approach allows for easy testing of different components and switching between characteristics without the need to navigate through all the simulation blocks.

```

1 |Ts=100e-6;|
2
3 |% COMPONENTS SETTINGS
4 |% Battery
5 |V_b = 32%48; % nominal voltage(V)
6 |C_b = 50%40; % rated capacity(Ah)
7
8 |% Supercapacitors
9 |V_sc = 270%291.6; % rated voltage
10 |C_sc = 55.4%15.6; % rated capacitance
11 |R_eq = 4e-3%150e-3; % Equivalent DC series resistance (Ohms)
12
13 |Vbus = V_sc*270/291.6;

```

(a)

```

42 |% CONVERTERS REFERENCES
43 |% fuel cell
44 |Ifcmaxd = 212/250*Ifcmax;
45 |VbusH = 297/270*Vbus;
46
47 |% battery
48 |Vconvbatt = 58/48*V_b;
49
50 |% LOAD DISCONNECT
51 |Vdisc = 200/270 * Vbus;
52 |IC = 1; % initial condition for the load (1=connected / 0=disconnected)
53
54 |% PROTECTIVE RESISTOR
55 |Vproth = 290/270 * Vbus;
56 |VprotL = 285/270 * Vbus;

```

(b)

```

15 |% STRATEGIES
16 |Vdcmin = Vbus*(1-10/270); % minimum bus voltage
17 |Idcmin = 140%73; % current added to recover from a too low Vdc
18 |Vdcmax = Vbus*(1+15/270); % maximum bus voltage
19 |Idcmax = 100%73; % current used to recover from a too high Vdc
20
21 |Ifcmax = 250%73;
22 |Ifcmin = 20%73;
23
24 |maxPIbatt = 80%73;
25 |minPIbatt = 20%73;
26
27 |% Classical PI
28 |SOC_ref = 60; % reference State Of Charge (%)
29 |SOC_limU = SOC_ref+1;
30 |SOC_limD = SOC_ref-1;
31
32 |Pbmax = 3400%73; % max battery power (w)
33 |Pbchar = 1500%73; % recharging battery power(w)
34
35 |Pfcmax = 8800%73; % maximum fuel cell power (w)
36 |Pfcmin = 850%73; % minimum fuel cell power (w)
37
38 |% EEMS
39 |DV_min=-2;
40 |DV_max=2;

```

(c)

**Figure 5.4:** Simulink initialization function

As can be observed, a rescaling approach was implemented for the simulation. This method adjusts certain parameters and recomputes others based on the relationships between components and their limits. However, it was a simple initial linear approach that failed to account for many important factors. Despite this, the function can still be used normally, allowing for the necessary values to be easily changed in order to test a new system. Since variables are being used, the

new parameters are automatically placed in the appropriate blocks. However, for simplicity and due to the similarities in values, the original simulation components will be retained for analyzing different strategies tailored to the WIG requirements.

Additionally, two other features should be highlighted:

- **Protective Resistor:** This component is used to prevent the voltage of the supercapacitor from rising too high.
- **Load Disconnect:** This feature monitors the common bus voltage and disconnects the load if  $V_{dc}$  falls below or exceeds safe levels, ensuring the system remains safe.

### 5.3 Strategies Settings

As mentioned in Section 3.2.2 the Classical PI works with a SOC reference value set to 60%. Instead the Memory-Based Hysteresis PI Control works a SOC range established by two thresholds set for the simulation at 59% and 61%.

To implement the MH-PI control, the configuration shown in Figure 5.5 was constructed. This setup includes switches that provide a simple method for controlling the signal, allowing for efficient management of the system across three distinct control regions.

For a more in-depth explanation of how this control strategy operates and its effectiveness in eliminating steady-state fluctuations, please refer to Section 3.3.

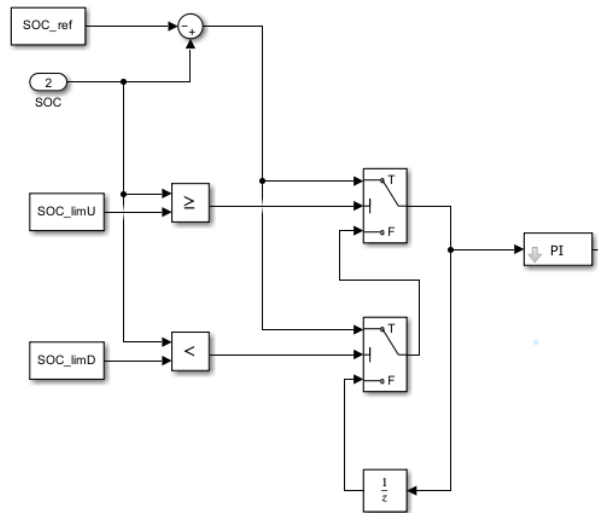


Figure 5.5: MH-PI switches configuration scheme

# Chapter 6

## Simulation Results

### 6.1 Power Scopes

To thoroughly examine the results of the simulations, several key factors were considered, with a focus on the power scope illustrated from Figure 6.1 to 6.7. This scopes highlights how different components contribute to the overall system performance and energy management throughout the simulation. The following elements were observed over time:

- **Load (yellow):** This represents the total power demand of the system, which remains consistent across all strategies. The Load serves as a baseline reference for comparing how effectively each energy source responds to the varying power requirements.
- **Fuel Cells Power (blue):** The power generated by the fuel cells is essential for understanding how much of the load demand is met by this primary energy source. Monitoring the fuel cells' power output provides insight into their efficiency and responsiveness under different operational conditions.
- **Battery Power (orange):** The battery plays a critical role in stabilizing the power supply, especially during peak loads or transitional phases. By analyzing the Battery Power, we can evaluate its contribution as a supplementary source and its impact on the overall system reliability.
- **Supercapacitors Power (green):** As an auxiliary energy source, the supercapacitors help manage short-term fluctuations and spikes in demand. The Supercapacitors Power plot reflects their quick response capabilities and their role in enhancing the system's transient performance.

By examining these components, we can better understand the dynamic interplay between them, enabling a more comprehensive assessment of the simulation strategies and their effectiveness in meeting the system's power requirements.

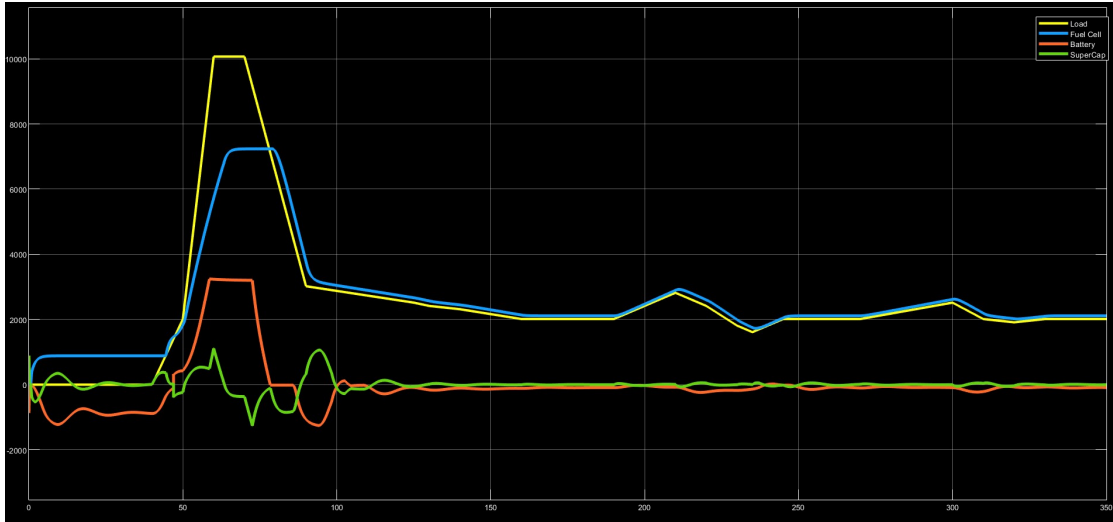


Figure 6.1: Power Scope - State Machine Control

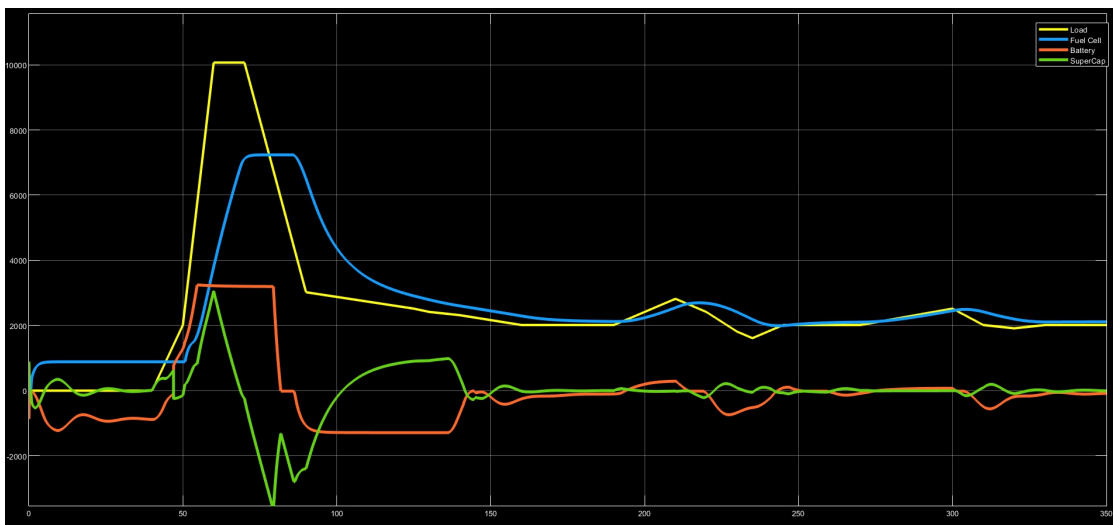


Figure 6.2: Power Scope - Frequency Decoupling and State Machine Control

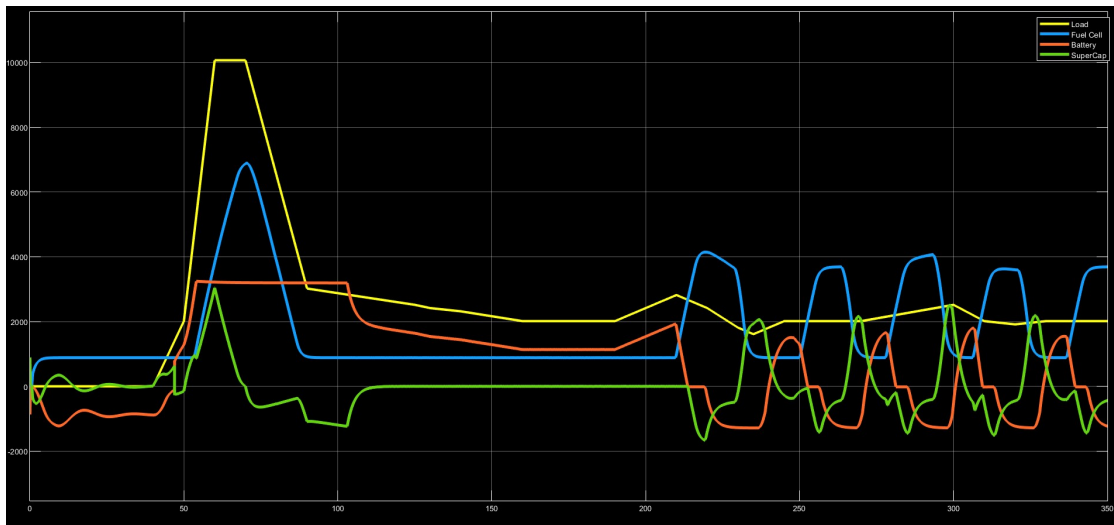


Figure 6.3: Power Scope - Classical PI Control

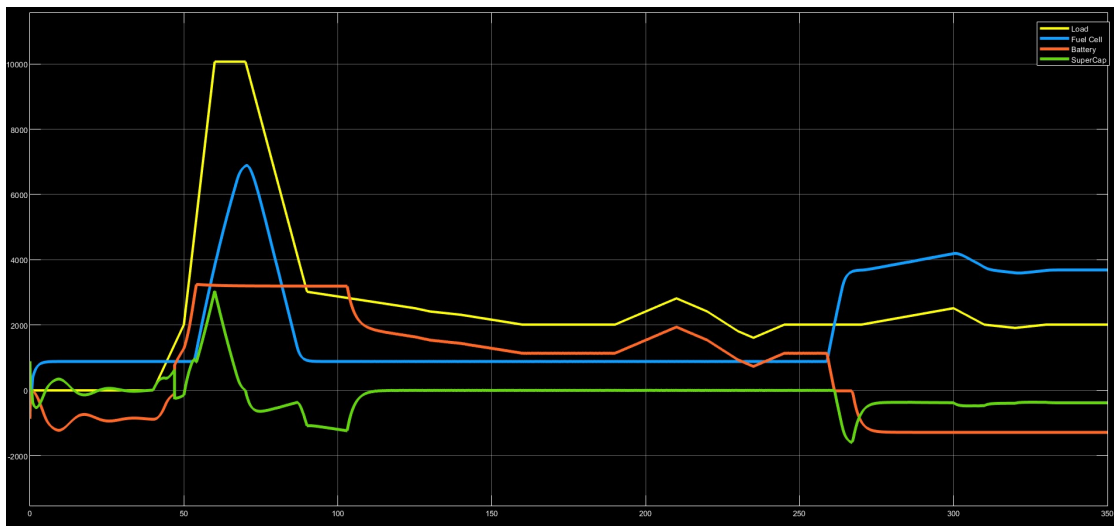


Figure 6.4: Power Scope - Memory-Based Hysteresis PI Control

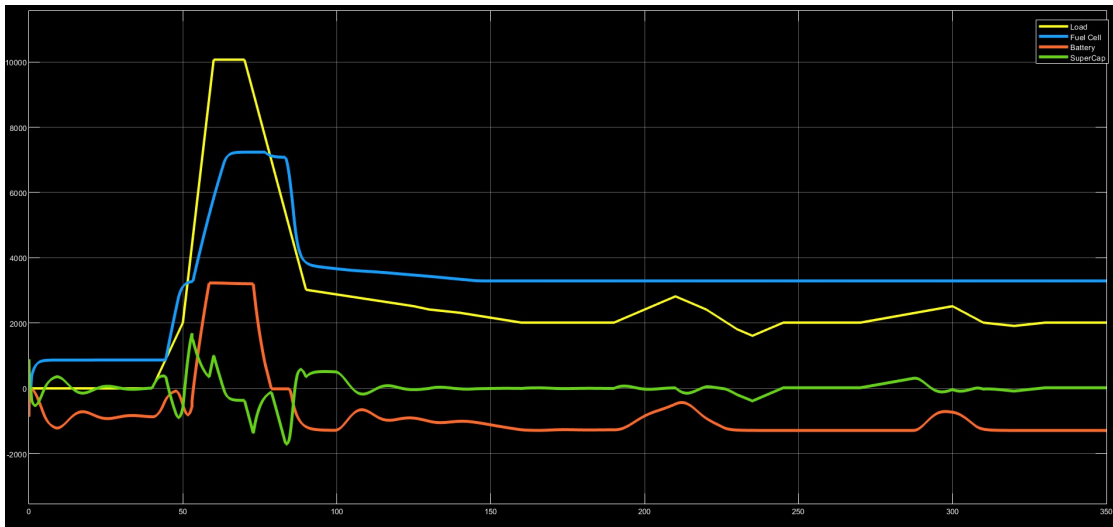


Figure 6.5: Power Scope - Fuzzy Logic Control

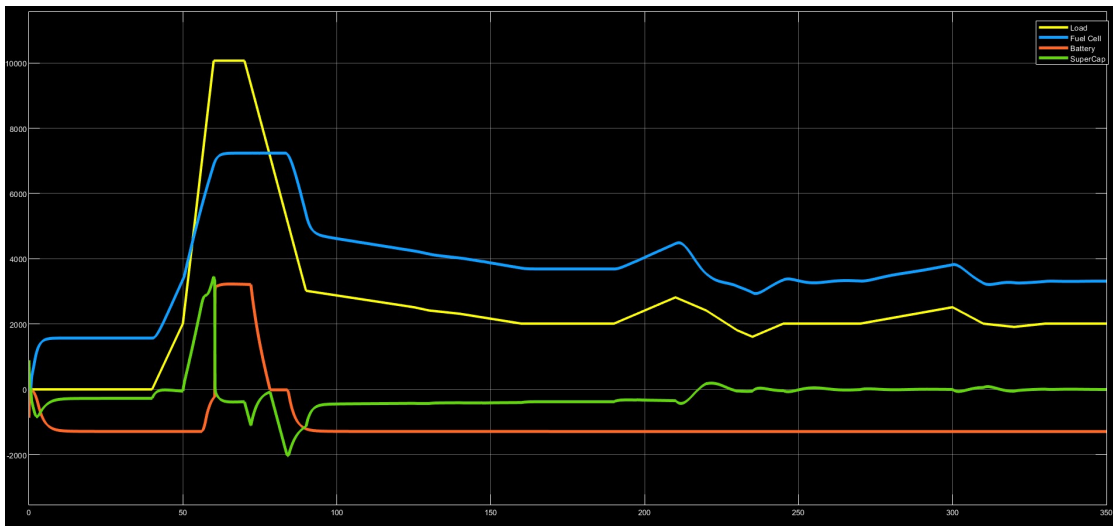


Figure 6.6: Power Scope - Equivalent Consumption Minimization Strategy

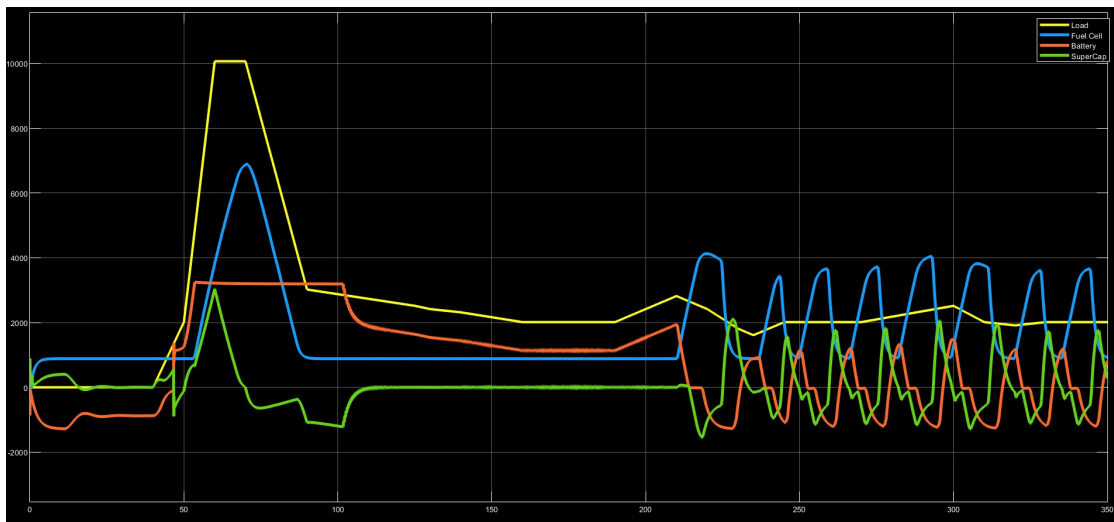


Figure 6.7: Power Scope - External Energy Maximization Strategy

## 6.2 Key-Parameters

The effectiveness of each strategy was assessed using a set of critical parameters, which are detailed in Table 6.1. These parameters provide a comprehensive overview of the system's operational characteristics and overall efficiency under varying conditions. The specific parameters analyzed include:

- **Fuel Consumption:** It measures the total amount of fuel used by the system. It is an essential metric for determining the energy efficiency of each strategy, as lower fuel consumption typically indicates a more sustainable and cost-effective approach.
- **Battery State of Charge (SOC) Range:** The SOC range of the battery is crucial not only for understanding its role in energy management but also for assessing its impact on battery lifecycle. Batteries with a narrower SOC range generally experience less stress, which can extend their overall lifespan by reducing the frequency and depth of charge-discharge cycles. Conversely, a wider SOC range might indicate a higher workload, potentially leading to accelerated aging and a reduced lifecycle if not managed properly.
- **Supercapacitor State of Charge (SOC) Range:** Like batteries, supercapacitors are also affected by their SOC range. Frequent and deep cycling can reduce their effective lifespan over time. However, supercapacitors are designed to handle rapid charge and discharge cycles more effectively than batteries. Evaluating their SOC range helps to determine how much of the transient load is managed by the supercapacitors, which can influence both their performance and longevity. A well-managed SOC range can enhance the supercapacitor's durability, contributing to improved system resilience.
- **System Efficiency:** This parameter provides a comprehensive view of the system's overall energy efficiency, taking into account all energy sources. A high system efficiency indicates effective energy utilization with minimal losses, which is essential for optimizing operational costs and ensuring long-term sustainability. In this case the overall efficiency was computed by comparing the power required from the load ( $P_{load}$ ) and the powers from each energy sources respectively.

$$\eta_{sys} = \frac{P_{load}}{P_{fc} + P_b + P_{sc}} \quad (6.1)$$

- **Supercapacitors Reaction Slope:** The reaction slope of the supercapacitor represents the rate at which it adjusts its power output in response to changes

in load demand. A steeper slope indicates a quicker response, which can be advantageous for handling sudden changes in power requirements.

- **Stability:** Stability is a critical factor, a strategy may show good performance in fuel consumption or system efficiency; however, it's important not to neglect stability since it can result in safety issues and additional stress on components."

By evaluating these parameters, it is possible to gain a more holistic understanding of each strategy's performance, allowing an identification of the most effective approach for optimizing system stability, efficiency, lifecycle of key components and responsiveness to dynamic load conditions.

	Fuel Consumption (g)	Battery SOC (%)	SuperCapacitors SOC(%)	Efficiency (%)	SuperCapacitors Reaction Slope (W/s)
<b>State Machine</b>	15.14	64÷65	92÷93	81.79	1354
<b>Classical PI</b>	10.59	60÷65	90÷94	78.89	3191
<b>MH-PI</b>	11.48	59÷65	90÷96	78.25	3191
<b>Fuzzy Logic</b>	19.97	64÷68	92÷93	75.35	1605
<b>Freq. Decoup.</b>	15.65	64÷65	90÷95	80.92	3207
<b>ECMS</b>	22.96	65÷69	92÷98	73.61	3513
<b>EEMS</b>	10.31	60÷66	90÷93	79.43	3160

**Table 6.1:** Simulation strategies comparison - key-parameters results

### 6.3 Observations

The Memory-Based Hysteresis PI Control, with the introduction of a narrow SOC range of just 2% effectively eliminated fluctuations during steady-state cruise mode, enhancing the overall stability and efficiency of the power system. This indicates a significant improvement over the Classical PI strategy, which exhibited undesirable fluctuations.

Based on the simulation results, the following observations can be made:

- **Supercapacitor Reaction Slope:** This parameter is crucial for applications on aircraft flying at low altitude as they need to be ready to react to potential hazards, especially for military applications, where rapid response to changing power demands is essential. The ECMS strategy exhibits the highest reaction slope, indicating its ability to respond quickly to load changes. However, this comes at the cost of the highest hydrogen consumption and lowest efficiency, making it less ideal for sustained operations.

- **Fuel Consumption:** The EEMS strategy demonstrated the lowest hydrogen consumption, which is advantageous for extending the operational range of the vehicle. However, its performance cannot be considered because of the presence of fluctuations at steady-state (Figure 6.7).
- **Efficiency and Stability:** The Frequency Decoupling strategy achieved the highest overall efficiency, closely followed by the State Machine and PIs strategies. The MH-PI strategy offers a good balance between fuel consumption, efficiency, and reaction slope, making it a strong candidate for practical implementation.

Considering all parameters, including the need for rapid response, fuel efficiency, and system stability, the Memory-Based Hysteresis PI Control emerges as the most balanced strategy. It provides a good compromise between reaction time, consumption, efficiency, and component wear and tear, making it suitable for agile maneuvers and dynamic power demands in WIG vehicles.

# Chapter 7

## Conclusions

In a world increasingly focused on addressing environmental challenges, the search for green solutions in mobility has gained significant momentum. The aviation and transportation sectors, responsible for a substantial share of global emissions, are now exploring alternative propulsion systems that reduce environmental impact while maintaining efficiency and performance. This study addresses this demand by investigating the design of a hybrid power system for an autonomous Wing-In-Ground Effect (WIG) vehicle, a concept that offers both high efficiency and sustainability in the field of transportation.

The study has explored various energy sources, including fuel cells, batteries, and supercapacitors, to develop an optimal hybrid power system configuration. By exploiting the unique capabilities of WIG vehicles, low-altitude, high-speed travel, and reduced energy consumption due to the ground effect, this research provides a foundation for innovative solutions in the pursuit of cleaner, more sustainable mobility. The combination of fuel cells with advanced energy management strategies ensures that the vehicle can achieve optimal performance while minimizing fuel consumption and emissions, thus contributing to the global shift towards greener mobility solutions.

Through simulations of different Energy Management System (EMS) strategies, including classical PI, state machine control, fuzzy logic, and others, the Memory-Based Hysteresis PI strategy emerged as the best overall solution. It effectively managed the balance between hydrogen consumption, power output, and component wear, outperforming both ECMS and EEMS in crucial aspects.

Field tests with scaled models confirmed the distinctive takeoff power profile of WIG vehicles, characterized by an initial power spike followed by a stabilization phase. This discovery provided a valuable basis for the system's validation and allowed for the fine-tuning of EMS strategies in simulations.

Despite the promising results, challenges remain in areas such as achieving smooth transitions out of the ground-effect zone and ensuring reliable energy

delivery during high-demand maneuvers. Future work should focus on further refinement of the control algorithms, investigating the potential of integrating renewable energy sources like solar panels, and extending flight stability beyond takeoff to cruise and landing phases.

In summary, this study demonstrates the potential of hybrid power systems in advancing WIG technology, highlighting how innovative EMS strategies and power electronics configurations can significantly improve the performance and sustainability of these vehicles for various applications.

## 7.1 Commercial Applications

WIG vehicles, with their ability to exploit the ground effect and achieve high speeds with low energy consumption, hold great promise for civilian transport, especially in coastal regions. Their capacity for intra-peninsular and coastal city-to-city connections makes them an ideal alternative to traditional maritime and air transport systems. The relatively simple infrastructure requirements and the ability to bypass congested traffic routes or lengthy ferry crossings could significantly enhance transportation efficiency in areas where large bodies of water or rugged terrain separate cities.

For instance, WIG vehicles could revolutionize intra-peninsular connections in regions like the Mediterranean or Southeast Asia, providing an efficient alternative to ferries or planes. The vehicles' ability to operate without the need for extensive runways or docking infrastructure allows them to service hard-to-reach areas, providing fast transport between coastal cities. This could have substantial implications for regional economies, tourism and emergency services, offering an eco-friendly and fast alternative for commuters, tourists and goods transport across water bodies or along coastal routes.

Furthermore, WIG vehicles' lower operational costs and reduced emissions align with the growing global trend towards green mobility. They offer the potential to reduce road congestion and decrease reliance on conventional fossil-fuel-powered transport systems, contributing to the development of cleaner transportation networks. Their use in goods transportation between coastal areas or even between islands could reduce the environmental footprint of logistics operations, enhancing supply chain efficiency while contributing to carbon reduction goals.

## 7.2 Military Applications

WIG vehicles hold considerable promise in the military sector due to their stealth, speed, and versatility in both maritime and coastal environments. Their low-altitude flight capabilities make them difficult to detect by radar and sonar, providing a

strategic advantage in numerous military operations. The hybrid power system, with its combination of fuel cells for endurance and batteries for high-demand situations, ensures that these vehicles can be deployed over long distances with minimal fuel consumption, making them ideal for high-stakes and covert missions.

In search and rescue operations, WIG vehicles can cover large areas of coastal or maritime regions quickly, deploying rescue personnel or supplies to areas that may be difficult to access by sea or air.

Additionally, WIG vehicles can serve a critical role in troop transportation and goods transport, offering high-speed alternatives to traditional naval or airborne methods. Their ability to transport personnel or cargo between naval ships and the coast without detection makes them invaluable for secure resupply missions or evacuations. Furthermore, in surveillance operations, WIG vehicles can patrol coastal and maritime borders effectively, operating for long periods with minimal energy consumption. This could aid in the detection of illegal activities, such as smuggling or unauthorized incursions into national waters.

# Chapter 8

## Future Work

The study is still in its early stages, and there are numerous opportunities for further improvement and exploration of the EMS approach for WIG military vehicles. Building on the insights gained from this research, the following directions are proposed for future exploration:

- **Feasibility of Flywheel Implementation:** One promising avenue for future research is the integration of Flywheel Energy Storage Systems (FESS) into the hybrid power architecture of WIG vehicles. Flywheels offer the potential to store and release large amounts of kinetic energy with high efficiency, particularly for short bursts of power. Their advantages include high power density, long cycle life, and the ability to quickly respond to sudden increases in power demand, which makes them an excellent candidate for high-power applications, such as WIG vehicle takeoff or rapid acceleration.

However, the feasibility of implementing flywheels into the current WIG vehicle configuration requires thorough investigation. Factors such as weight, size, rotational stability, and energy recovery efficiency need to be carefully considered. Flywheels could complement the use of batteries and supercapacitors, providing a mechanical alternative for energy storage that is less reliant on chemical degradation over time. Exploring the optimal integration point within the hybrid power system, possibly as an auxiliary power source for transient loads, will be a critical step in evaluating the viability of flywheels in this context.

- **Implementation of Solar Panels:** The integration of solar panels into the energy system of WIG vehicles offers significant potential for enhancing both the range and sustainability of these vehicles. Solar panels could be installed on the surface of the WIG vehicle's fuselage and wings, providing an additional source of clean energy, particularly during daylight operations in coastal or

sunny regions. The added solar energy could reduce reliance on fuel cells and batteries, further minimizing fuel consumption and emissions. Future work should explore the technical challenges of incorporating solar panels into the vehicle design, such as optimizing panel placement to maximize energy capture without compromising aerodynamics or adding significant weight.

In terms of energy management, the Energy Management System (EMS) would need to be adapted to prioritize solar energy usage when available, switching between fuel cells, batteries, and solar power based on real-time conditions.

- **Parameter Variation for Different Scales:** The results obtained in this study are based on simulations and field tests using scaled models of WIG vehicles. However, when moving from scaled models to full-scale operational vehicles, key parameters such as power demand, energy storage capacity, and load requirements will change significantly. Therefore, future work should focus on how these parameters vary across different scales and how this affects the sizing and configuration of power systems.

For example, larger WIG vehicles designed for cargo or military applications may require significantly higher peak power during takeoff, necessitating more robust fuel cells, larger batteries, or additional energy storage systems. Conversely, smaller, lightweight WIG vehicles for civilian transport may prioritize weight reduction and energy efficiency, leading to different system optimization goals.

- **Development of New Strategies and Improvement of Existing Ones:** While the MH-PI control strategy has shown promise in managing the energy flow efficiently, there is still room for improvement and the development of new energy management strategies. Dynamic control strategies that respond to real-time changes in operational conditions, such as load fluctuations, battery health, and environmental factors, could offer better performance than static or semi-static approaches.

One potential enhancement to the Memory-Based Hysteresis PI Control (MH-PI) strategy is the introduction of dynamic thresholds that are updated online during vehicle operation. Instead of using fixed upper and lower limits for the battery's state of charge (SOC). For instance, during high-power demands, the SOC thresholds could be adjusted to prioritize battery discharge, while during periods of low demand, the system could optimize fuel efficiency by favoring fuel cell operation.

- **Alternative Configurations:** In addition to enhancing existing control strategies, exploring alternative configurations of the hybrid power system is another important direction for future work.

For example, different converter topologies, such as multi-input converters that manage both batteries and supercapacitors, could simplify the system while maintaining flexibility. Additionally, fully integrating flywheels or solar panels into the energy management system might require alternative power architectures to ensure optimal energy flow.

Future studies should also explore more modular designs that allow for swapping or upgrading components based on specific mission requirements. This would enable WIG vehicles to be highly adaptable, with their power systems configured to meet the demands of various operational scenarios, whether a short-range civilian mission or a long-range military reconnaissance.

By developing new strategies, refining existing ones, and exploring alternative configurations, future research can continue to optimize the energy systems of WIG vehicles, enhancing their performance, adaptability, and sustainability.

# Appendix A

## Field Tests Scale Models Details

Below are the data for the Albatros model (Figure A.1 and Figure A.2) and Mistral model (Figure A.3)

### ALBATROSS MEASUREMENTS

Part	Length (cm)	Breadth (cm)	Height (cm)
Fuselage	175	65	60
Wing	150	100	40
Tail	70	125	55

Figure A.1: Albatros dimensional details

**REQUIRED ON-BOARD HARDWARE COMPONENTS**

Sensor	Model	Manufacturer	Weight (g)	Notes
IMU	STIM300	Novatel	55	
	TAC-450-320 IMU	Emcore	70	
	POLAR-300-AHRS-IMU	UAV Navigations	76	With GNSS system
GPS	AsteRx-m3 Pro+	Septentrio	26	
	simpleRTK3B Heading	Ardusimple		
Battery	LiPo battery 4S 14.8v-5000mAh	Gens ace	437	2 units
<b>Total Weight-</b>			<b>976</b>	

<b>FOR INITIAL TESTING- AVAILABLE HARDWARE FROM INESC-TEC</b>				
IMU+GPS	CubePilot Cube Flight Controller	PX4 Autopilot	75	Standalone flight controller with inbuilt IMU, Compass, altimeter and other sensors
<b>Total Weight-</b>			<b>949</b>	

IMU	Ellipse-N	Sbg Systems	49	Inertial Navigation System with internal GNSS
-----	-----------	-------------	----	---

**Figure A.2:** Albatros hardware components details



**EKRANOPLANO RC “MISTRAL”  
SEMIMAQUETA RC A ESCALA DEL EKRANOPLANO “AIR FISH 8”**

**CARACTERÍSTICAS:**

**Modelo fabricado con poliuretano y maderas de haya y contrachapado.  
Diseño fabricado de forma compacta sin partes desmontables.  
salvo el empenaje de cola (derivas y estabilizador que a su vez forman una pieza compacta).**

**Envergadura: ..... 150 cm.  
Eslora casco: .....100 cm.  
Longitud total: .....115 cm.  
Cuerda máx alas: .....56 cm.  
Cuerda mín. alas: .....18 cm.  
Peso de los motores:.....312 g. (dos motores)  
Peso de los variadores:.....144 g. (dos variadores)  
Peso de los servos: ..... 48 g. (cuatro microservos)  
Peso de las baterías:..... 495 g.  
Peso plomo (lastre): ..... 257 g.  
Peso del modelo en vacío:..... 1.500 g.  
Peso total del modelo en orden  
de vuelo: ..... 2.756 g.**

**EQUIPACIÓN PROPULSIÓN:**

**Baterías LiPo 4S - 14,8V - 5000 mAh - 60C.....x2  
Motores Bruhsless DYS 1100 KV.....x2  
Variadores brushless M-H 80A .....x2  
Servos micro MG90S 4.8V6.0V.....x4  
Emisora FUTABA SKYPORTE-T4YF-2.4 GHz.....x1**



Figure A.3: Mistral datasheet

# Appendix B

## Components Datasheets

### B.1 Fuel Cell

Horizon Fuel Cell Technologies[18] - H-Series Fuel Cell Stacks / H-3000

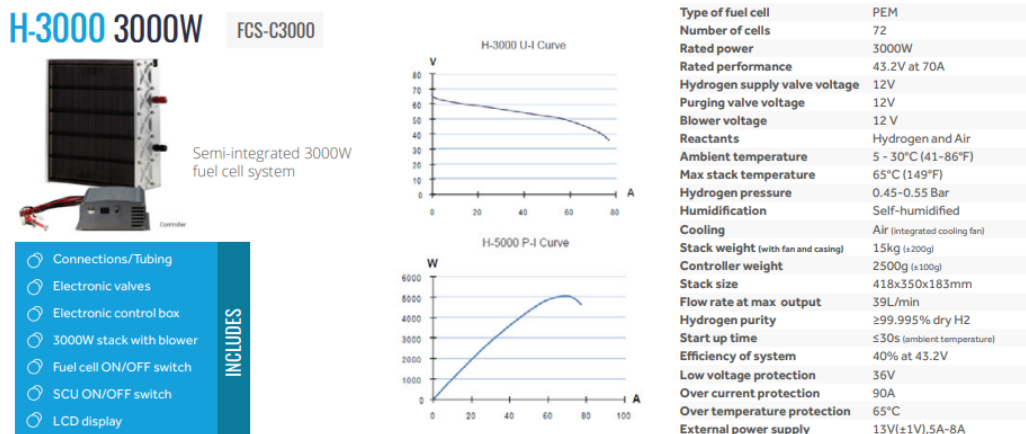


**Figure B.1:** H-Series fuel cell stacks / H-3000 datasheet

Supposedly there's an error in the P-I curve, the H5000 P-I characteristic has been reported instead the H3000 one.

## B.2 Solid State Battery

The German startup HPB (High Performance Battery)[22] is developing solid-state batteries (SSBs) that possess the characteristics and potential to revolutionize the future of battery technology.

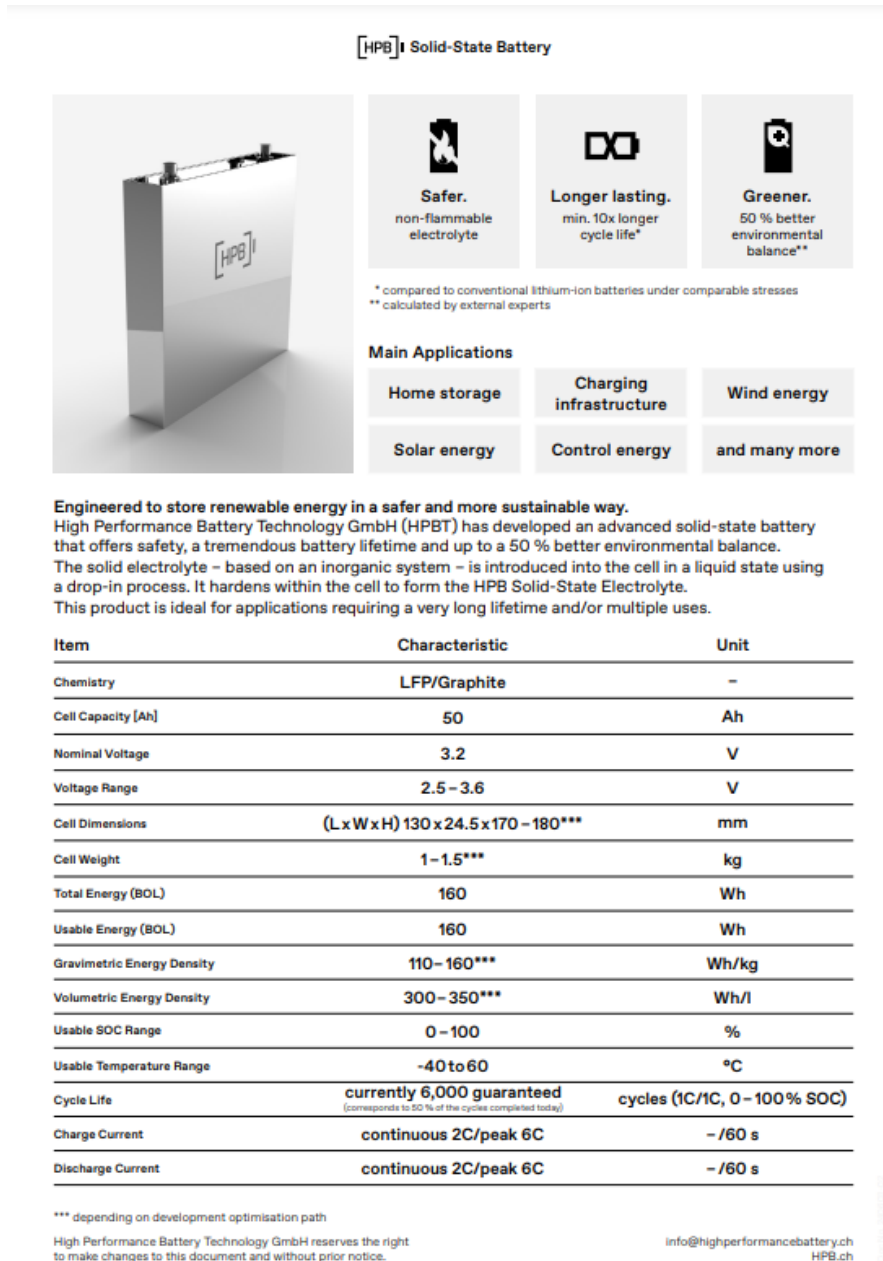


Figure B.2: High Performance Battery - SSB datasheet, page 1/3

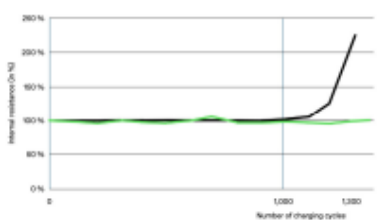


Measurements

Status 05/2024

**HPB Technology – Engineered to store renewable energy in a safer and more sustainable way.**  
 To ensure a neutral assessment, HPB activities are consistently monitored scientifically by external experts.

**HPB Solid-State Battery | Cycle Life Characteristics**  
 (>12,500 and ongoing) 1C/1C, 0-100 % SOC, RT



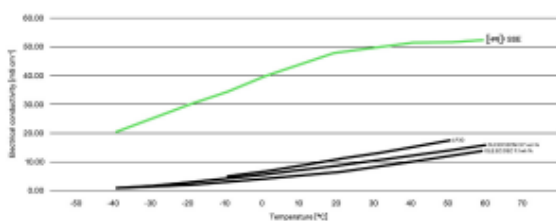
**>12,500 and ongoing**

While conventional lithium-ion batteries have to be replaced after about approx. 1,250 charging cycles\* – with hourly charging and discharging – the HPB Solid-State Battery currently has at least 12,500 charging cycles, with a comparable load.

Since these cycle life test cells have not yet reached the end of their life, this number will continue to increase steadily.

\*Source: <https://www.sciencedirect.com/science/article/pii/S2666546821055355>

**HPB Solid-State Electrolyte | Conductivity Characteristics**  
 temperature range: from -40°C to 60°C

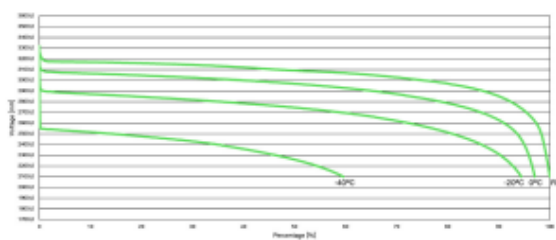


**Higher conductivity over the entire temperature spectrum**

Compared to the liquid electrolytes commonly used today, the HPB Solid-State Electrolyte has an enormously improved conductivity. This is decisive for the available power from the battery cell. The HPB Solid-State Electrolyte shows an absolutely higher conductivity at minus 40 °C than conventional liquid electrolytes at their optimum at plus 60 °C.

Source: [1] J. Landbeck, H. A. Gasteiger, J. Electrochem. Soc. 2019, 166(6), A3379–A3387 (URL: <https://pubs.aip.org/jes/article/166/6/3379/23579124>) [2] T.R. Jow, K. Xu, C. Santhan, M. Ue (Ed.), Electrolytes for Lithium and Lithium-Ion Batteries, 2016, Modern Aspects of Electrochemistry Vol. 58, Springer, New York. [3] T. B. Reddy (Ed.), Linden's Handbook of Batteries, 2015, 4th ed., McGraw-Hill Education Ltd.

**HPB Solid-State Battery | Discharge Capacity Characteristics**  
 Charge: CC-CV 0.5 C 3.6V, 0.1 C cut-off at 25 °C (RT)/Discharge: 1C cut-off at 25 °C (RT)/0°C/-20°C/-40°C



**High performance at low temperatures**

Where other batteries without external battery heating give up, the HPB Solid-State Battery is still in its comfort zone: Even at -20 °C, the extractable capacity is more than 90 % – tested at a robust discharge rate (1C). This is a real game changer for the use of batteries in winter.

If you would like to carry out your own measurements with HPB Technology, please contact FEV Europe GmbH.

Rémi Stohr  
 stohr@fev.com  
 +49 (0)151 42 62 4464

FEV Europe GmbH  
 Neuenhofstraße 181  
 52078 Aachen

High Performance Battery Technology GmbH reserves the right to make changes and/or additions to this document and without prior notice.

info@highperformancebattery.ch  
 HPB.ch

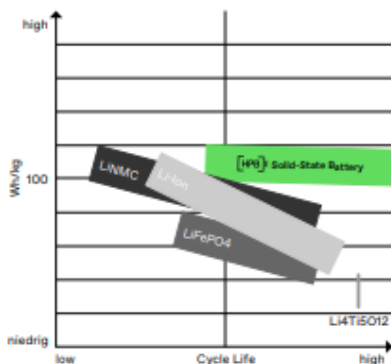
Figure B.3: High Performance Battery - SSB datasheet, page 2/3



**HPB Technology in technology comparison.**

The following charts provide a rough indication of how the outstanding properties of HPB Technology can be categorised in comparison to the current competition.

**HPB Solid-State Battery | Wh/kg and cycle life**  
technology comparison with Li-Ion, LNMCC, LiFePO4 and Li4Ti5O12



**Longer lasting and smaller dimensions.**

A key parameter of battery storage systems is their specific energy: the maximum amount of electrical energy that can be stored in relation to the battery mass, expressed in watt hours per kilogramme (Wh/kg).

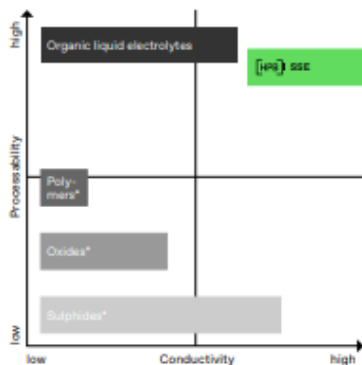
With stationary storage systems, the specific energy generally decreases with increasing cycle life, which must be compensated for by larger battery storage systems depending on the application – with consequences for resource requirements and the environment.

Compared to other long-life storage systems, the HPB Solid-State Battery also has significantly higher specific energies in the long term. A battery storage system with HPB Technology can therefore be dimensioned significantly smaller for an identical application.

When selecting a storage system, the specific energy parameter must be considered in the context of the other battery characteristics. For example, the fast-charging capability (C-rate) is another lever for resource efficiency. We have clearly summarised these relationships in our white paper „Rightsizing“.

Source: [https://www.highperformancebattery.ch/global/downloads/21008\\_impulses\\_for\\_the\\_energy\\_transition\\_-\\_rightsizing\\_-\\_but\\_the\\_right\\_way.pdf](https://www.highperformancebattery.ch/global/downloads/21008_impulses_for_the_energy_transition_-_rightsizing_-_but_the_right_way.pdf)

**HPB Solid-State Electrolyte | Conductivity and processability**  
technology comparison with polymers, oxides and sulphides as well as conventional organic liquid electrolytes



**More conductive and easy to process.**

The HPB Solid-State Electrolyte (SSE) achieves outstanding conductivity values across the entire temperature spectrum and therefore not only outperforms conventional organic liquid electrolytes, but also the conductivity values of other solid-state electrolytes (polymers, oxides and sulphides).

Compared to other solid-state electrolytes (polymers, oxides and sulphides), however, the HPB Solid-State Electrolyte is much easier to produce, as it can be manufactured due to known production processes from conventional lithium-ion batteries with liquid electrolytes.

In a two-stage process during cell production, the starting materials for forming the HPB Solid-State Electrolyte are first introduced from the production of the raw electrode to the electrode stack. By adding the final components in liquid form, similar to the liquid electrolyte filling of conventional lithium-ion batteries, the chemical reaction to form the HPB Solid-State Electrolyte in the battery cell begins.

The conductivities and the specific challenges of industrial production of the other solid ion conductors (polymers, oxides and sulphides) are clearly described in the Fraunhofer Institutes “Solid-state batteries Roadmap 2035+“ study.

\*Solid-state electrolyte

Source: [https://www.ifa.fraunhofer.de/content/dam/ifa/documents/ict/2022-SSB\\_Roadmap.pdf](https://www.ifa.fraunhofer.de/content/dam/ifa/documents/ict/2022-SSB_Roadmap.pdf)

Figure B.4: High Performance Battery - SSB datasheet, page 3/3

## B.3 Supercapacitors

Skeleton Technologies[23], SkelCap Supercapacitors - SCX5000

PRELIMINARY DATA SHEET



# SkelCap<sup>+</sup>

supercapacitor

- + Capacitance 5000 F
- + Extreme power density
- + Durable and safe aluminum casings
- + Weldable terminals
- + High cycle life > 1,000,000 cycles
- + High temperature tolerance (operating and storage)
- + German quality
- + RoHS compliant




General	Value	Unit
Rated voltage $V_R$	3	V
Rated capacitance	5000	F
Initial capacitance, typical	5200	F
DC 10ms ESR rated	0.14	m $\Omega$
DC 1s ESR rated	0.20	m $\Omega$
ESR (IEC62391-1), rated	0.20	m $\Omega$
Maximum peak current, for 1 second <sup>1,9</sup>	3.8	kA

Power	Value	Unit
<b>Nominal power, calculated from 10ms ESR (for comparison)</b>		
Power, matched impedance <sup>5</sup>	16.1	kW
Specific power, matched impedance <sup>6</sup>	28.4	kW/kg
Power density, matched impedance <sup>7</sup>	41.2	kW/L
<b>Nominal power, calculated from 1s ESR (for engineering)</b>		
Power, matched impedance <sup>5</sup>	11.2	kW
Specific power, matched impedance <sup>6</sup>	19.9	kW/kg
Power density, matched impedance <sup>7</sup>	28.9	kW/L

Standards and certifications	Value
Vibration Specification	ISO 16750-3, Table 12 Table 14
Certifications	RoHS

Physical parameters	Value	Unit
Mass, typical ( $\pm$ 3-8 g, from small to large size)	0.565	kg
Volume	0.390	L
Diameter ( $\pm$ 0.2 mm, including label), D1	60.2	mm
Length ( $\pm$ 0.3 mm), L1	138	mm
Terminal diameter, $\varnothing 2$	12	mm
Terminal length, L2	3.2	mm

Temperature and Life	Value	Unit
<b>Operating temperature range</b>		
Minimum	-40	$^{\circ}$ C
Maximum	+65	$^{\circ}$ C
<b>Storage temperature range (uncharged)</b>		
Minimum	-40	$^{\circ}$ C
Maximum	+50	$^{\circ}$ C
<b>Life</b>		
Capacitance decrease 20% from rated value; resistance increase 100% from rated value		
Storage life @ RT, uncharged	10	Years
Cyclelife @ RT, between $V_R$ and $V_R/2$	1,000,000	Cycles



Copyright © 2024 Skeleton Technologies GmbH. All rights reserved.  
 02-DS-211228-SKELCAP-SCX-11  
 Page 1/2

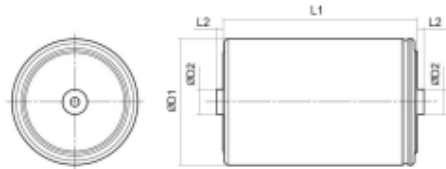
Figure B.5: SCX5000 datasheet, page 1/2

Energy	Value	Unit	Thermal (based on DC 1s ESR)	Value	Unit
Energy <sup>2</sup>	6.3	Wh	Thermal resistance given $\Delta T = 30^{\circ}\text{C}$ , $R_{th}$	3	$^{\circ}\text{C}/\text{W}$
Specific energy <sup>3</sup>	11.1	Wh/kg	Thermal capacitance, $C_{th}$ , typical	634	J/ $^{\circ}\text{C}$
Energy density <sup>4</sup>	16.0	Wh/L	Max continuous current <sup>10</sup> , $\Delta T = 15^{\circ}\text{C}$ <sup>4</sup>	158	A
			Max continuous current <sup>10</sup> , $\Delta T = 30^{\circ}\text{C}$ <sup>4</sup>	224	A
			Max continuous current <sup>10</sup> , $\Delta T = 40^{\circ}\text{C}$ <sup>4</sup>	258	A

**Safety**

**Short circuit current** 21.4 kA  
 (For informational purposes - do not use as operating current.)

(1) Maximum peak current (1 sec)  $= \frac{\frac{1}{2} CV}{C \cdot ESR + 1s}$  (2)  $E_{max} = \frac{\frac{1}{2} CV^2}{3600}$  (3)  $E_{max} = \frac{\frac{1}{2} CV^2}{3600 \cdot mass}$   
 (4)  $E_{max} = \frac{\frac{1}{2} CV^2}{3600 \cdot volume}$  (5)  $P_{max} = \frac{V^2}{4 \cdot ESR}$  (6)  $P_{max} = \frac{V^2}{4 \cdot ESR \cdot mass}$   
 (7)  $P_{max} = \frac{V^2}{4 \cdot ESR \cdot volume}$  (8)  $I_{max} = \sqrt{\frac{\Delta T}{ESR + R_{th}}}$



(9) The stated maximum peak current should not be exceeded during use. If the limit is to be exceeded by the customer, Skeleton must be consulted beforehand and give approval for the exceeded power load. Typical value represents the mean production sample value. Rated value represents the absolute minimum capacitance or maximum ESR value of production sample.  
<sup>4</sup>Power values calculated using DC 10ms ESR = AC 100Hz.

**Standard markings**

- Name of manufacturer, part number, serial number, rated voltage
- Rated capacitance, negative and positive terminals, warning marking
- Total energy in watt-hours
- Electrolyte material used

**Notes**

- Testing instructions available on [www.skeletontech.com](http://www.skeletontech.com)
- All information provided on this data sheet and all subsequent ultracapacitors sales and testing are subject to Standard Terms of Service (ToS) available on [www.skeletontech.com](http://www.skeletontech.com), document General Terms of Sale for Skeleton Technologies GmbH.



Figure B.6: SCX5000 datasheet, page 2/2



# Bibliography

- [1] A. A. Abdelhafez and A. J. Forsyth. «A Review of More-Electric Aircraft». In: *AEROSPACE SCIENCES & AVIATION TECHNOLOGY* (2009, Volume 13) (cit. on p. 2).
- [2] *Boeing 787 Dreamliner - Electrical system*. URL: <https://787updates.net/wairplane.com/787-Electrical-Systems/787-Electrical-System#:~:text=The%20787%3A%20A%20more%2Delectric%20system&text=Benefits%20of%20the%20787's%20innovative,wiring%20than%20on%20the%20767> . (cit. on p. 2).
- [3] *F-35 Lightning II - Electro-Optical Targeting System (EOTS)*. URL: <https://www.lockheedmartin.com/en-us/products/f-35-lightning-ii-eots.html> (cit. on p. 2).
- [4] J. Gordon Leishman. *Introduction to Aerospace Flight Vehicles*. Embry-Riddle Aeronautical University, 2023 (cit. on pp. 4, 6, 7).
- [5] *WigetWorks*. URL: <https://www.wigetworks.com/> (cit. on p. 5).
- [6] *DARPA Requests Information For Wing-in-Ground Effect Aircraft For the U.S. Military*. URL: <https://www.navalnews.com/naval-news/2021/08/darpa-requests-information-for-wing-in-ground-effect-aircraft-for-the-u-s-military/> (cit. on p. 9).
- [7] S. N. Motapon. «Design and simulation of a fuel cell hybrid emergency power system for a more electric aircraft: evaluation of energy management schemes». PhD thesis. École de technologie supérieure Université du québec, 2013 (cit. on pp. 10, 28, 36, 43).
- [8] K. Erhan and E. Özdemir. «Prototype production and comparative analysis of high-speed flywheel energy storage systems during regenerative braking in hybrid and electric vehicles». In: *Journal of Energy Storage* (2021, Volume 43) (cit. on p. 11).
- [9] A. Rupp, H. Baier, P. Mertiny, and M. Secanell. «Analysis of a flywheel energy storage system for light rail transit». In: *Energy* (2016, Volume 107, Pages 625-638) (cit. on p. 11).

- [10] M. Esfahanian, A. Safaei, H. Nehzati, V. Esfahanian, and M. M. Tehrani. «Matlab-based modeling, simulation and design package for Electric, Hydraulic and Flywheel hybrid powertrains of a city bus». In: *International Journal of Automotive Technology* (2014, Volume 15, pages 1001-1013) (cit. on p. 11).
- [11] B. Thormann, P. Puchbauer, and T. Kienberger. «Analyzing the suitability of flywheel energy storage systems for supplying high-power charging e-mobility use cases». In: *Journal of Energy Storage* (2021, Volume 39) (cit. on p. 11).
- [12] Z. Yang, G. Sun, P. Behrens, P. A. Østergaard, M. Egusquiza, E. Egusquiza, B. Xu, D. Chen, and E. Patelli. «The potential for photovoltaic-powered pumped-hydro systems to reduce emissions, costs, and energy insecurity in rural China». In: *Energy Conversion and Management: X* (2021, Volume 11) (cit. on p. 11).
- [13] B. Xiang, X. Wang, and W. O. Wong. «Process control of charging and discharging of magnetically suspended flywheel energy storage system». In: *Journal of Energy Storage* (2022, Volume 47) (cit. on p. 11).
- [14] T. Dragičević, S. Bo, E. Schaltz, and J. M. Guerrero. «Flexible local load controller for fast electric vehicle charging station supplemented with flywheel energy storage system». In: *IEEE International Electric Vehicle Conference (IEVC)* (2014) (cit. on p. 11).
- [15] S. Khosrogorji, M. Ahmadian, H. Torkaman, and S. Soori. «Multi-input DC/DC converters in connection with distributed generation units». In: *Renewable and Sustainable Energy Reviews* (Volume 66, December 2016, Pages 360-379) (cit. on p. 14).
- [16] A. Priyanto, A. Maimum, S. Noverdo, J. Saeed, A. Faizal, and M. Waqiyuddin. «A Study on Estimation of Propulsive Power for Wing in Ground Effect (WIG) Craft to Take-off». In: *Journal Teknologi* (2012) (cit. on p. 18).
- [17] H. Huang, J. Meng, Y. Wang, F. Feng, L. Cai, J. Peng, and T. Liu. «A comprehensively optimized lithium-ion battery state-of-health estimator based on Local Coulomb Counting Curve». In: *Applied Energy* (2022, volume 322) (cit. on p. 20).
- [18] *Horizon Fuel Cell Technologies*. URL: <https://www.horizonfuelcell.com/> (cit. on pp. 22, 66).
- [19] C. K. Chan, H. Peng, G. Liu, K. Mellwrath, X. F. Zhang, R. A. Huggins, and Y. Cui. «High-performance lithium battery anodes using silicon nanowires». In: *Nature Nanotechnology* · (January 2008) (cit. on p. 24).

- [20] H. Li, A. Ravey, A. N'diaye, and A. Djerdir. «Equivalent consumption minimization strategy for hybrid electric vehicle powered by fuel cell, battery and supercapacitor». In: *IECON* (2016 - 42nd Annual Conference of the IEEE Industrial Electronics Society) (cit. on p. 36).
- [21] *MathWorks - Energy Management Systems for a Hybrid Electric Source (Application for a More Electric Aircraft)*. URL: [https://it.mathworks.com/help/sps/ug/energy-management-systems-for-a-hybrid-electric-source-application-for-a-more-electric-aircraft.html?searchHighlight=Energy%20Management%20Systems%20for%20a%20Hybrid%20Electric%20Source%20%28Application%20for%20a%20More%20Electric%20Aircraft%29&s\\_tid=srchtitle\\_support\\_results\\_1\\_Energy%20Management%20Systems%20for%20a%20Hybrid%20Electric%20Source%20%2528Application%20for%20a%20More%20Electric%20Aircraft%2529](https://it.mathworks.com/help/sps/ug/energy-management-systems-for-a-hybrid-electric-source-application-for-a-more-electric-aircraft.html?searchHighlight=Energy%20Management%20Systems%20for%20a%20Hybrid%20Electric%20Source%20%28Application%20for%20a%20More%20Electric%20Aircraft%29&s_tid=srchtitle_support_results_1_Energy%20Management%20Systems%20for%20a%20Hybrid%20Electric%20Source%20%2528Application%20for%20a%20More%20Electric%20Aircraft%2529) (cit. on p. 43).
- [22] *High Performance Battery*. URL: <https://www.highperformancebattery.ch/en/> (cit. on p. 67).
- [23] *Skeleton Technologies*. <https://www.skeletontech.com/en/skelcap-supercapacitors> (cit. on p. 70).